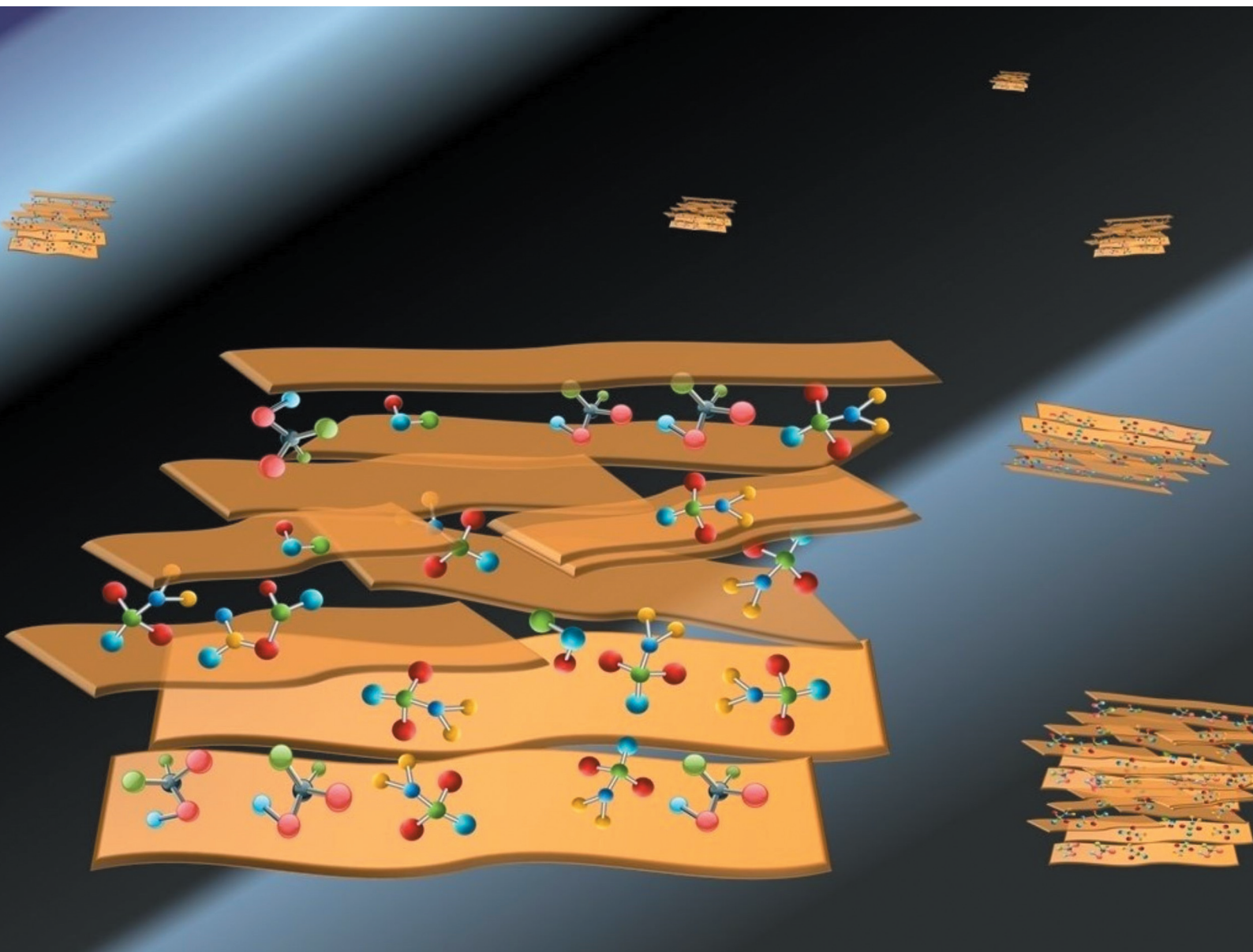


# Nanoscale

rsc.li/nanoscale




ISSN 2040-3372



Cite this: *Nanoscale*, 2023, **15**, 18959

## MXenes vs. clays: emerging and traditional 2D layered nanoarchitectonics

Eduardo Ruiz-Hitzky  <sup>\*a</sup> and Cristina Ruiz-Garcia  <sup>b</sup>

Although MXene materials are considered an emerging research topic, they are receiving considerable interest because, like metals and graphene, they are good electronic conductors but with the particularity that they have a marked hydrophilic character. Having a structural organization and properties close to those of clay minerals (natural silicates typically with a lamellar morphology), they are sometimes referred to as “conducting clays” and exhibit colloidal, surface and intercalation properties also similar to those of clay minerals. The present contribution aims to inform and discuss the nature of MXenes in comparison with clay phyllosilicates, taking into account their structural analogies, outstanding surface properties and advanced applications. The current in-depth understanding of clay minerals may represent a basis for the future development of MXene-derived nanoarchitectures. Comparative examples of the preparation, and studies on the properties and applications of various nanoarchitectures based on clays and MXenes have been included in the present work.

Received 24th June 2023,  
Accepted 19th September 2023

DOI: 10.1039/d3nr03037g

rsc.li/nanoscale

### 1. Introduction

Research on 2D solids represents a very important area to achieve nanoscale functional materials with extraordinary properties capable of reaching advanced applications in many diverse research fields. In this way, inorganic layered solids such as transition metal oxides and chalcogenides (TMD), car-

<sup>a</sup>Materials Science Institute of Madrid, CSIC, c/Sor Juana Inés de la Cruz 3, 28049 Madrid, Spain. E-mail: eduardo@icmm.csic.es

<sup>b</sup>Chemical Engineering Department, Faculty of Science, c/Francisco Tomás y Valiente 7, Universidad Autónoma de Madrid, 28049 Madrid, Spain



**Eduardo Ruiz-Hitzky**

*Eduardo Ruiz-Hitzky, Ad Honorem Research Professor at the Instituto de Ciencia de Materiales de Madrid (CSIC), has conducted pioneering research during the past 50 years on nanostructured systems including functional hybrids, nanocomposites and nanoarchitectures based on silica/silicates (clays), 2D metal oxides and chalcogenides, graphene and, recently, MXenes, publishing ca. 300 publications. The chair of*

*leading conferences (e.g. EUCHEM, RSC Materials Discussions, co-organizer of ACS Symposia), he has received various international distinctions such as the “STAS Award”, Académie Royale de Belgique (Belgium, 1975), the “AIPEA Medal” (Japan, 2005) and the “Bailey Distinguished member Award”, the highest honor of The Clay Minerals Society (USA, 2020).*



**Cristina Ruiz-Garcia**

*Cristina Ruiz-Garcia obtained her PhD in Chemistry at the Autonomous University of Madrid (UAM), Spain, in 2017. She has developed her research career linked to different research institutions in academia and industry. Currently, she belongs to the Chemical Engineering Department of the UAM as postdoctoral Marie Skłodowska Curie fellow. The main aim of her activities is focused on the study of nano-materials such as graphene and clays, among others, and their application in environmental catalysis.*



**Table 1** Comparative characteristics of various 2D inorganic solids (\* mixed ionic-electronic conductivity)

| Physicochemical characteristics          | MXenes | Clay minerals | V <sub>2</sub> O <sub>5</sub> ·nH <sub>2</sub> O | Li <sub>x</sub> MoS <sub>2</sub> | Graphite/graphene |
|--|--------|---------------|--|----------------------------------|-------------------|
| Inorganic layered (2D) solids            | ✓      | ✓             | ✓  | ✓                                | ✓                 |
| Elemental layers of nanometric thickness | ✓      | ✓             | ✓  | ✓                                | ✓                 |
| Hydrophilic character                    | ✓      | ✓             | ✓  | ✓                                | ✗                 |
| Stable colloidal water dispersion        | ✓      | ✓             | ✓  | ✓                                | ✗                 |
| Intercalation ability                    | ✓      | ✓             | ✓  | ✓                                | ✓                 |
| Electronic conductivity                  | ✓      | ✗             | *  | ✓                                | ✓                 |

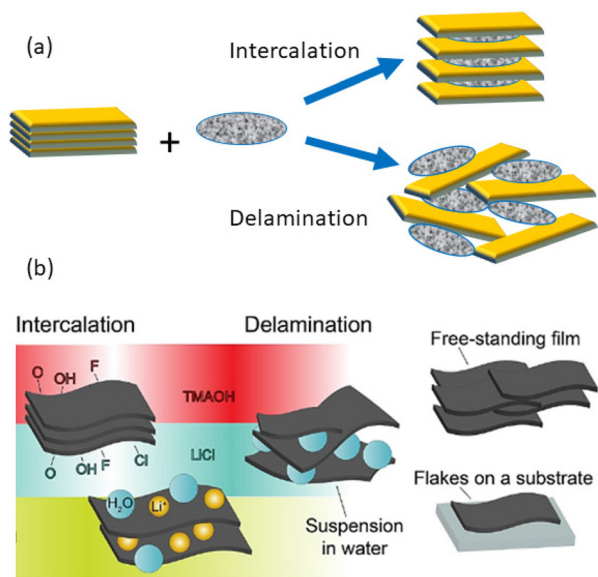
bides and nitrides, phosphates and phosphonates, graphite and graphene-like materials, layered double hydroxides (LDHs), layered alkaline silicates and silicic acids, as well as a large group of phyllosilicates belonging to the family of clay minerals, have received much attention in recent years due to their outstanding physicochemical properties.

The comparative physicochemical characteristics of a selection of 2D solids (MXenes, clay minerals, vanadium pentoxide xerogel, the lithiated phase of molybdenum disulphide and graphene/graphite) are grouped in Table 1. All of them have the ability to intercalate very diverse chemical species, as well as the capability to delaminate and/or exfoliate in single layers (nanosheets or monolayers) (Fig. 1), thus contributing to the assembly of diverse chemical species, including polymers and nanoparticles, generating a large family of nanoarchitected materials.<sup>1–9</sup> This characteristic of 2D solids makes it possible to prepare many diverse hybrid materials and nanoarchitectures by the intercalation of neutral and ionic species<sup>3,5,6,10–16</sup>

or by assembly with inorganic nanoparticles of a very distinct nature.<sup>17–21</sup>

MXenes and 2D clay minerals are amenable for forming stable dispersions of delaminated solids in the form of flakes constituted by single layers or as few-layer materials showing remarkable characteristics that can be different from those in their condensed state.<sup>18</sup> MXenes (M<sub>n+1</sub>X<sub>n</sub>T<sub>x</sub>) discovered in the past decade<sup>22</sup> represent a wide family of 2D solids derived from ternary transition metal carbides and/or carbonitrides named “MAX phases” of M<sub>n+1</sub>AX<sub>n</sub> general formula where “M” represents a transition metal of elements in the periodic table from columns 3 and 7 (e.g., Ti) and “A” belongs to elements from columns 13 to 16 (e.g., Al). “X” represents carbon and/or nitrogen (carbides, nitrides or carbonitrides) and OH, O or F species resulting from HF treatment and located as surface terminations, called “T” groups, responsible for the hydrophilic properties possessed by MXenes (Fig. 2d and e).<sup>23</sup> MXenes are receiving tremendous interest due to their exceptional physicochemical properties endowing advanced technological applications and constituting therefore marked progress in the field of new functional materials.<sup>22–27</sup> MXenes are also known by the nickname of “conductive clays”,<sup>†</sup> apparently because of their similar characteristics to clay minerals.<sup>28</sup> The appellation of clays as MXenes would be attributed to their similarity in terms of physicochemical properties like those of some 2D clays. In some cases, they have been called “carbide clays” (see for instance the paper by Ghidui *et al.*<sup>28</sup>) which, in our opinion, is not entirely correct, since “clays” is a term mainly associated with silicates and other small-size particles present in the geosphere. Even more, publications on typical MXene topics have been recently presented at leading clay conferences, as for instance “The 2023 60th Clay Minerals Society Meeting”.<sup>29</sup> From our perspective, it should be considered useful and enriching for clay scientists to know studies related to 2D solids of a different nature from clays, as well as other materials related to clay minerals, including also small colloidal particles, such as silica, iron oxides, *etc.*, and, therefore, MXenes, in our opinion, may be included here.

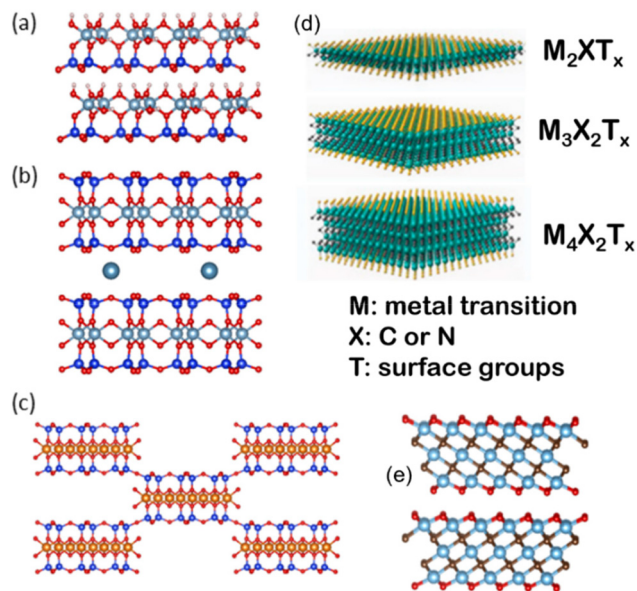
The traditional term “clays” refers to raw materials or rocks from sedimentary deposits, but it is often used in the literature as an abbreviation for “clay minerals”, although the latter



**Fig. 1** Scheme showing the general ability of 2D solids to intercalate organic and inorganic species by delamination/restacking processes to generate functional nanoarchitectures (a). In the particular case of MXenes (b), the figure details the steps to intercalate and delaminate these 2D solids in water suspensions, leading to free-standing colloidal films and flake deposition on a planar substrate. This last image is adapted with permission from Sarycheva and Gogotsi, *Chem. Mater.*, 2020, 32(8), 3480–3488. Copyright 2020, American Chemical Society.

<sup>†</sup>See for instance the two most cited articles searching by “Clay\* and Intercalation” as the topic entries in Clarivate-WoS, which are related to MXenes, both published in 2014 with a total of *ca.* 7000 citations. The total number of publications on clays is 52 680 and 9710 on MXenes in the 2019–2022 period.





**Fig. 2** Crystal structures of a selection of clay minerals (a–c) based on Al- and Mg-phylosilicates of 1:1 type such as kaolinite (a), 2:1 type such as montmorillonite (b) and sepiolite (c), and 2D MXenes (d and e) of  $M_{n+1}X_nT_x$ , as a general formula (M = early transition metal; X = C and/or N, and  $T_x$  = OH, F surface terminations) (d). The value  $n = 1-4$  indicates the number of transition metal layers (and carbon and/or nitrogen layers), i.e.,  $Ti_3C_2T_x$  ( $n = 2$ ) (e). The (a), (b), (c) and (e) figures have been built using VESTA 3 software,<sup>33</sup> and (d) has been adapted from Wyatt *et al.*, 2D MXenes: Tunable Mechanical and Tribological Properties, *Adv. Mater.*, 2021, 33, 2007973, Wiley.

should be considered more appropriate for an accurate designation of this type of silicate.<sup>30</sup> Clay minerals occur in nature as a result of the chemical weathering of silicate rocks, so the chemical composition of clays is not well defined in natural deposits. This is a limiting factor for their use in advanced applications, including the preparation of organic–inorganic hybrid materials and diverse functional nanoarchitectures. Despite their costs compared with natural clays, synthetic clay minerals with a well-designed composition and structure appear as an alternative to provide advanced functional materials for new applications that require well-defined and homogeneous samples.<sup>31</sup> In addition, clay minerals are composed mainly of silica, alumina or magnesia or both and water, but iron or titanium could substitute for aluminum and/or magnesium in varying ratios, and appreciable quantities of inorganic ions like  $Na^+$ ,  $K^+$ ,  $Mg^{2+}$  and  $Ca^{2+}$  are frequently present as well.<sup>32</sup>

Typical clay minerals belong to several families that among other 2D silicates include from one side kaolinite and halloysite aluminosilicates, organized as a layered superposition, each composed of 1:1 of two sheets of tetrahedral and octahedral components ( $SiO_4$  and  $Al_2O_3$ , respectively), as well as smectites (*e.g.*, montmorillonite and hectorite) and vermiculites. These two latter groups are called 2:1 clays because they are structurally composed of layers comprising two tetrahedral sheets sandwiching one octahedral sheet. These 1:1 and 2:1

clay minerals are present under the general aspect of platelets, except halloysite clay that can also be present as nanotubes. Finally, there is a group of clay minerals such as sepiolite and palygorskite, with alternating structural blocks (2:1 type) and tunnels showing a fibrous-like morphology. A representative selection of the structures of these types of clay is shown in Fig. 2.

As far as their structural arrangement is concerned, it can be comparatively summarized that clays result from a combination of silica tetrahedra and aluminum or magnesium octahedra forming sheets. The isomorphic substitutions can generate negative charges compensated by exchangeable cations in the interlamellar region. On the other hand, MXenes have a completely different composition: they are aluminum carbides derived from the so-called MAX phases by the extraction of these atoms described above in arranged sheets with a delocalization of electrons in the lamellae that ensures an electrical conductivity comparable to that of graphene but absolutely different from that of clays.

Numerous review articles have been published to date dealing separately with very different aspects of the 2D traditional clays and the emerging MXenes. To the best of our knowledge, there is currently no publication dealing with the comparative aspects considered here with both types of layered solid.

The main goal of this critical review is to highlight the recent advances of MXenes in the development of new functional nanoarchitected materials in connection with traditional clay minerals and their derivatives. Since the latter have been extensively studied in the past decades to develop advanced nanoarchitected materials, this generated knowledge can be considered in many aspects as models to be applied in a useful way for the future development of new functional 2D MXene materials, based on the close relationship between these two types of solid.

## 2. Preparation and comparative physicochemical characteristics of clays and MXenes

Clay minerals are naturally occurring silicates present in soils. Although some of them can also be synthesized at the laboratory and industrial scales, their most widespread use refers to minerals present in the abundant deposits available worldwide.<sup>31</sup> The advantage of using synthetic clays should be mainly related to their potential use in advanced applications, facilitating the preparation of samples of controlled composition, as well as new crystalline phases. In addition, there is the possibility to modify them by introducing specific properties and also to prepare high-purity materials of interest in several fields, for example, in biomedicine.

However, as already mentioned, the most economical and sustainable way to obtain clays with a certain degree of purity is to exploit their sedimentary deposits, located in countless



places around the Earth. In fact, life on Earth is linked to the presence of clays and therefore of water, which is necessary for its geofomation. The use of clays for the preparation of advanced materials requires a previous purification of the raw clay, generally by sedimentation techniques, trying to eliminate common impurities such as quartz, mica, carbonates, iron oxides, organic matter, *etc.*, which usually accompany natural clay silicates as minor components. In the frequent case of the purification of smectite clays (*e.g.* montmorillonite) it is important to proceed in a first step to the saturation of the silicate with  $\text{Na}^+$  ions by ion exchange processes to prepare the sodium homoionic clays, which are generally used with a known particle size distribution around the micrometer diameter.<sup>34</sup> As for carbides, unlike the abundant clay silicates on Earth, only a few exoplanets appear to consist of a mantle dominated by carbides rather than silicates.<sup>35</sup> Carbides related to the MXene family derive from the “MAX” phases (hexagonal ternary two-dimensional materials, *vide supra*), which in turn are usually synthesized by solid state reactions at high temperatures under an inert atmosphere, appearing as the most competitive method compared with alternative ways such as isostatic pressing, sputtering, or spark plasma sintering.<sup>36</sup> For example, the typical procedure for the synthesis of the  $\text{Ti}_3\text{AlC}_2$  typical MAX phase consists of the treatment of stoichiometric amounts of Ti, Al and C (as graphite), and grinding in ball mill equipment before reacting at 1400–1700 °C for 1–4 h in a tubular furnace under an Ar flux. This procedure is considered the best synthesis approach, as it represents a relatively low-

cost and scalable process compared with the alternative methods.<sup>36,37</sup> Table 2 shows several strategies of MXene synthesis from MAX phases, mostly selected from the work of Chen and co-workers.<sup>38</sup> The etching of “A” layers (*e.g.*, Al in  $\text{Ti}_3\text{AlC}_2$ ) by immersion in concentrated HF at room temperature was the first method for MXene preparation reported by Naguib and co-workers in 2011.<sup>22</sup>

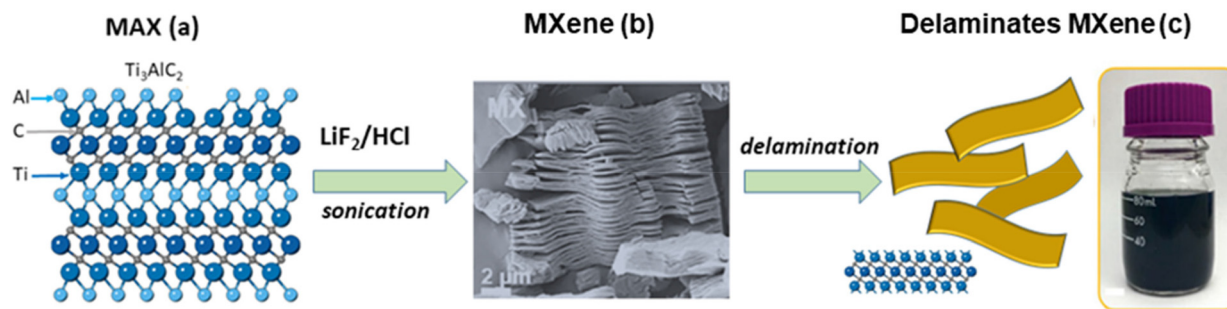
The resulting suspension was washed with water followed by centrifugation to separate the remaining solids, which after ultrasonication in methanol gave rise to flakes containing the carbide nanosheets by exfoliation of the MXenes remaining in suspension (Fig. 3).

To avoid the use of concentrated HF, which is a toxic and aggressive reagent that requires careful safety precautions, alternative MXene synthesis approaches have been developed up to the present. In this way, Ghidui *et al.*<sup>28</sup> reported in 2014 the first synthesis of an MXene using LiF dissolved in concentrated HCl at moderate temperature. Although extended periods of reaction time were required, the use of concentrated HF solutions was avoided. Despite the fact that the latter procedure is safer than the former, it still produces small amounts of HF, so it is of great interest to develop alternative methods that completely avoid the use of fluorinated compounds, preventing the formation of terminations “T” as F bonded to the resulting MXene sheets. In this regard, Li *et al.*<sup>42</sup> used a hydrothermal etching route by autoclaving at 270 °C in highly concentrated NaOH. Following this approach, a lot of work has been developed but nevertheless according to

**Table 2** Chemical synthesis approaches of MXenes from MAX phases (based on ref. 38–41) TMAOH and TBAOH correspond to tetramethylammonium hydroxide and tetrabutylammonium hydroxide, respectively

| Synthesis strategies                           | Involved reagents  | Materials characteristics   | Advantages   | Drawbacks   |
|--|--|---|--|---|
| HF etching                                     | HF   | • Accordion-like structure  | • Effective for most MAX   | • Dangerous operation<br>• Cannot be peeled                   |
| Fluoride-based acid etching                    | $\text{LiF}/\text{NaF}/\text{KF} + \text{HCl}$<br>$\text{NH}_4\text{HF}_2$ | • Abundant F terminations<br>• Clay-like MXene<br>• Large interlayer spacing                              | • High yield<br>• Relatively safe<br>• Direct ultrasonic peeling       | • Long etching time<br>• Introducing fluoride salt impurities |
| Alkaline solution etching                      | NaOH or TMAOH  | • Few –F terminations<br>• Accordion-like structure only with –O, –OH terminations                        | • No risk of acid corrosion<br>• Free of F terminations                | • NaOH: severe etching conditions<br>• TMAOH: HF pretreatment |
| HCl-based hydrothermal etching                 | HCl (aq)   | • Layered structure with –Cl and –O terminations  | • Easy experimental operation<br>• Fluorine-free                       | • Severe etching conditions<br>• Rely on the DFT predictions  |
| Lithiation-expansion: microexplosion mechanism | Lithium ions   | • Single- or few-layer structure without –F terminations  | • Easy and safe synthesis<br>• Free of –F terminations                 | • Low productivity<br>• Consume resources                     |
| Water free etching                             | $\text{NH}_4\text{HF}_2$ in organic solvents                               | • Accordion-like structure<br>• Abundant –F terminations  | • Compatible with organic systems<br>• Delamination by ultrasonication | • Long etching time<br>• Tedious washing steps                |
| Molten salts                                   | $\text{CuCl}_2 : \text{NaCl} : \text{KCl}$                                 | • Delamination with TBAOH<br>• Abundant –Cl terminations  | • Fluorine-free process<br>• Free of –F terminations                   | • High temperature ( <i>ca.</i> 700°) required                |
| Ionic liquids                                  | Imidazolium-based ionic liquids  | • Accordion-like morphologies but different from $\text{Ti}_3\text{C}_2\text{T}_x$ produced by HF etching | • Fast and HF-free process avoiding the use of any acid                | • High cost and toxicity of ionic liquids                     |





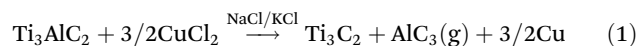
**Fig. 3** Scheme showing the synthesis of stable colloidal delaminated MXene (c) from Ti<sub>3</sub>AlC<sub>2</sub> MAX phase (a) treated with HF. The accordion-like structure of the intermediate MXene can be observed (SEM image) (b). Figures are in part reprinted: (a) from Michatowski *et al.*, Oxycarbide MXenes and MAX phases identification using monoatomic layer-by-layer analysis with ultralow-energy secondary-ion mass spectrometry, *Nat. Nanotechnol.*, 2022, 17, 1192–1197, Springer Nature; and (b) from Li *et al.*, MXene-Enhanced Chitin Composite Sponges with Antibacterial and Hemostatic Activity for Wound Healing, *Adv. Healthcare Mater.*, 2022, 11, 2102367, Wiley.

Chen *et al.*<sup>38</sup> the advantages of the use of NaOH at elevated temperatures, which involves potential high safety risks too, are not clear. Thus a safer organic alkali etching procedure was proposed by Xuan *et al.* using TMAOH to successfully etch MAX phases like Ti<sub>3</sub>AlC<sub>2</sub>.<sup>43</sup> In this case a previous step is required, applying a first treatment of the MAX phase with HF at low concentration followed by Al etching by the TMAOH, leading to MXenes with Al(OH)<sub>4</sub><sup>−</sup> species as terminal groups. The fact that the use of HF remains necessary here, coupled with the caustic and toxic nature associated with alkylammonium hydroxides, again points to the potential risks associated with current MXene synthesis procedures. In this context numerous researchers around the world continue studying safer and more sustainable synthesis methods.

It should be noted that fluorine is present in MXenes from HF or LiF treatments whereas the F occasionally detected in natural clays is due to its geof ormation or introduced during its synthesis in the laboratory or in industry. Fluorine in clay minerals structurally substitutes hydroxyl groups very strongly bound to Mg<sup>2+</sup> or Al<sup>3+</sup> ions located in the octahedral layers of the clays, where it is immobilized. For example, the mineral hectorite, as well as the synthetic clay marketed as LAPONITE®, have a relatively high fluorine content, which is not capable of participating in interactions with substances placed in contact with clays,<sup>44</sup> again making these silicates safe for humans.

To address experimental conditions that avoid the use of HF for MXene synthesis, alternative methods such as HCl-based hydrothermal etching, halogen etching, *in situ* electrochemical synthesis, CVD processes, molten salts, waterless etching, lithium insertion, ionic liquids, *etc.*, have been proposed.<sup>38</sup> For instance, etching of Ti<sub>3</sub>AlC<sub>2</sub> with ammonium bifluoride (NH<sub>4</sub>HF<sub>2</sub>) in organic solvents of high polarity, such as dimethyl sulfoxide (DMSO), *N,N*-dimethyl formamide (DMF), propylene carbonate, *etc.*, appears to be a safer procedure resulting in hybrid materials with increased interlayer spacing and high −F terminations.<sup>45</sup> A drawback of the latter procedure is the long etching time (196 h) required at present to generate MXenes. An alternative fluorine-free procedure for

the synthesis of MXenes consisting of treatments with CuCl<sub>2</sub> in molten salts has been recently proposed by Liu *et al.*<sup>40</sup> In this way, the Ti<sub>3</sub>AlC<sub>2</sub> MAX phase reacts with molten salts (CuCl<sub>2</sub>:NaCl:KCl), facilitating the Al etching in a redox process with the formation of copper metal. The AlCl<sub>3</sub> formed in gas phase at the high temperature of the molten salts (*ca.* 700 °C) produces the expansion of the MXene layers (eqn (1)), which can be easily delaminated in a further treatment with tetrabutylammonium hydroxide (TBAOH) under ultrasonication.



A different synthetic procedure for the preparation of MXenes avoiding the use of any acid, including HF, has been recently reported by Husmann *et al.* using fluorine-containing ionic liquids and water.<sup>46</sup> The use of imidazolium-based ionic liquid containing BF<sub>4</sub><sup>−</sup> or PF<sub>6</sub><sup>−</sup> anions in the presence of water leads to the selective removal of Al, the ionic liquid intercalating between the MXene layers favoring their delamination in a very fast process compared with etching processes involving acidic reagents.

Finally, another interesting approach for the synthesis of fluorine-free MXenes is the so-called “lithiation–expansion–microexplosion mechanism” recently reported by Sun *et al.*<sup>47</sup> As an example, Li from a lithium foil as a cathode is electrochemically inserted into Ti<sub>3</sub>AlC<sub>2</sub>, and the further ultrasonication in water generates a microexplosion reaction producing the etching and generation of Ti<sub>3</sub>C<sub>2</sub>T<sub>x</sub> MXene. In our opinion, the latter mechanism could be compared with the formation of the lithiated phases of transition metal dichalcogenides (TMDs), where Li is spontaneously inserted into the van der Waals gap of the TMD.<sup>48</sup> Interestingly, 2D dichalcogenides, such as MoS<sub>2</sub>, can be easily intercalated through a redox reaction with lithium reagents (*e.g.* *n*-butyllithium) in anhydrous solvents (*e.g.* *n*-hexane), giving rise to Li<sub>x</sub>TMD compounds.<sup>48</sup> Lithiated phases like Li<sub>x</sub>MoS<sub>2</sub> react violently with water, generating H<sub>2</sub> and inducing TMD delamination in d-MoS<sub>2</sub> single layers, which could re-stack entrapping diverse



oxyethylene compounds such as crown-ethers and cryptand macrocycles, as well as poly(ethylene oxide) (PEO), leading to nanocomposites possessing controlled ion-mobility.<sup>15,49</sup> Interestingly, these approaches could be of interest for possible application to MAX phases, trying to develop new procedures for the preparation of MXene functional nanoarchitectures. More recently, Rasamani and co-workers enlarged this approach, reporting MoS<sub>2</sub> intercalation through the chemical insertion of Li<sup>+</sup> following exchange with NH<sub>3</sub> and NH<sub>4</sub><sup>+</sup> taking place in the interlayer region, with a second step of TMD exfoliation followed by restacking in the presence of diverse guest compounds.<sup>50</sup> From these results, it may be considered that, in theory, MAX phases could foreseeably show a similar behavior to TMDs against lithiation processes. However, to date no reference to this effect has been identified by searching databases such as WoS-Clarivate.

Regarding clay minerals, swelling of smectites and vermiculites followed by delamination is also well known in these charged 2 : 1 phyllosilicates, particularly in homoionic samples exchanged with high hydration energy cations, such as Li<sup>+</sup>, Na<sup>+</sup> and other alkaline ions. The extent of the swelling mainly depends on the location and density charge in the silicate microcrystals, as well as on the nature of the interlayer exchangeable cations. The swelling of smectites (montmorillonite, hectorite, *etc.*) exchanged with Li<sup>+</sup> and Na<sup>+</sup> ions leads to colloidal dispersions when water is spontaneously incorporated, provoking the delamination/exfoliation of individual clay layers (nanosheets) leading to stable colloidal dispersions.<sup>34</sup> Vermiculites, which are similar in structure to smectites but have a higher density charge and often occur as macroscopic crystals, are also typical swelling clay minerals, especially when exchanged with Li<sup>+</sup> or alkylammonium cations (*i.e.*, *n*-propyl and *n*-butyl-ammonium)<sup>51</sup> or even with certain amino acids such as L-ornithine.<sup>52</sup> They give rise to macroscopic 2D swollen materials that generate visible vermicular (accordion-like) arrangements and lead to gels by delamination when they are dispersed in water or in solutions of very low salt concentration. These accordion-like morphologies, typically observed in the early swelling phases produced by vermiculites, are also observed (*vide supra*) to some extent in the lithiated MAX phases (Fig. 3), appearing as intermediate in the formation of delaminated MXenes.<sup>53</sup>

The delamination of certain 2D solids into single-sheet or few-layer materials remaining as stable colloids in aqueous dispersions facilitates the formation of diverse nanoarchitectures following restacking processes. This approach was initially applied in clay-derivatives, the entrapment of molecules, polymers and nanoparticles being mainly characterized by spectroscopy, microscopy and diffraction techniques, including small-angle X-ray scattering and high-angle neutron diffraction. Compared with 2 : 1 phyllosilicates (*i.e.*, smectite and vermiculite clays), the family of kaolinite 1 : 1 aluminosilicates (kaolinite, nacrite, dickite and halloysite) can also be exfoliated/delaminated but with great difficulty. In this case, partial delamination can be reached by applying different routes from the usual ones for smectite and vermiculite. In

fact, 1 : 1 clay minerals can be hardly delaminated by mechanical exfoliation by grinding and assisted sonication.<sup>54</sup>

Table 3 compares various physicochemical characteristics of both smectite clay minerals and MXenes. They show many similar aspects, although decisive details related to their inherent properties, such as chemical composition and electronic conductivity, indicate that these two types of 2D material could be considered for similar or complementary applications.

Certain physicochemical properties of clays highlighted above have led to their traditional and historical use since antiquity in pottery, ceramics and glass, building, paper making, polymer reinforcement, medical and pharmaceutical uses, decoration and artistic developments, among other applications. Clay minerals are nowadays receiving a wide range of uses in industry, engineering and the environment and more recently in nanotechnology, as summarized in Table 4, including a comparison with some recent MXene applications. In fact, clays have been used for thousands of years, even in daily life applications, while MXenes have only been known for a few years, but there have been rapidly developed high-tech advances in functional materials and nanoarchitectonic fields.

A common feature of MXenes and clays is their marked hydrophilic character, forming stable colloids (Table 3). Clay particles are easily dispersed in water, salt and molecular solutions, producing stable hydrogels with interesting rheological properties. In particular, smectite clay minerals such as montmorillonite exchanged with high hydration energy ions (*i.e.*, Na<sup>+</sup>, Li<sup>+</sup>) give rise to delaminated silicate dispersions in water, which can self-organize *via* face-edge aggregation forming reversible thixotropic gel networks useful for a wide range of applications, for instance paints, petrochemicals, pesticides, food, cosmetics, pharmaceuticals and regenerative medicine.<sup>55–59</sup> Applications related to food, human and animal health are possible due to the biocompatible character of clay minerals, which have been extensively used for medicinal purposes since prehistoric times.<sup>60–62</sup> Fibrous clay minerals such as sepiolite could also be disaggregated in water by the application of high-speed shear forces or sonomechanical

**Table 3** Comparison between the physicochemical properties of clay minerals and MXenes

| Chemical composition                     | Silicates | Carbides/nitrides/<br>carbonitrides |
|--|-----------|-------------------------------------|
| Aspect ratio                             | High      | High                                |
| 2D inorganic solids                      | ✓         | ✓                                   |
| Elemental layers of nanometric thickness | ✓         | ✓                                   |
| Hydrophilic character                    | ✓         | ✓                                   |
| Stable water dispersions                 | ✓         | ✓                                   |
| Ion-exchange capacity                    | ✓         | ✓                                   |
| Swelling and intercalation ability       | ✓         | ✓                                   |
| Delamination ability                     | ✓         | ✓                                   |
| Electronic conductivity                  | No        | ✓                                   |
| Biocompatibility                         | ✓         | ✓                                   |
| Natural origin                           | ✓         | No                                  |
| Synthesis preparation                    | ✓         | ✓                                   |
| Cost                                     | Low       | High                                |



**Table 4** Selected examples of the comparison of applications from nanoarchitected materials derived from clay minerals and MXenes

| Advanced applications  | Clay-based materials  | MXene-based materials   |
|--|---|---|
| <ul style="list-style-type: none"> <li>• Adsorption and heterogeneous catalysis</li> <li>• Molecular separation: water and air purification. Environmental protection and remediation</li> </ul> | <ul style="list-style-type: none"> <li>• Air and water purification by adsorption of common pollutants<sup>14,69</sup></li> <li>• Pillared-clay materials by insertion of Al<sub>13</sub><sup>7+</sup> polycations: intercalated clay catalysts<sup>70,71</sup></li> <li>• Clay modifications by assembly of semiconducting NP (TiO<sub>2</sub>, ZnO...) for photocatalytic reactions<sup>20</sup></li> <li>• Uptake of heavy and radioactive metal ions using nanoscale modified clay minerals<sup>72,73</sup></li> <li>• Magnetic adsorbents based on ferrofluid infiltration<sup>74</sup></li> <li>• Clay-based bionanocomposites for oil-spill remediation<sup>75</sup></li> <li>• Wastewater and sewage treatments involving agricultural, urban and industrial wastewater treatments<sup>76–79</sup></li> </ul> | <ul style="list-style-type: none"> <li>• MXene-hybrids for environmental remediation<sup>80</sup></li> <li>• Al<sub>13</sub>-Ti<sub>3</sub>C<sub>2</sub>T<sub>x</sub> pillared-MXene by insertion of Al<sub>13</sub><sup>7+</sup> polycations</li> <li>• MXenes-TiO<sub>2</sub> for photocatalysis<sup>24,81,82</sup></li> <li>• MXene-nanocomposites for heavy metal and radionucleid removal<sup>83,84</sup></li> <li>• MXenes-magnetite with enhanced photothermal activity<sup>85</sup> and radionucleid removal<sup>86</sup></li> <li>• MXene-based membranes and sponges for oil-spills<sup>87,88</sup></li> <li>• MXene-based nanoarchitectures for wastewater disposal<sup>89,90</sup></li> </ul> |
| <ul style="list-style-type: none"> <li>• Membranes, ionic and electronic conductors and sensor devices</li> <li>• Corrosion protection</li> </ul>  | <ul style="list-style-type: none"> <li>• Membranes for ion-recognition and oxygen sensors<sup>91</sup></li> <li>• Bionanocomposites for ion-detection<sup>92–94</sup></li> <li>• Organoclays as components of (bio)sensors<sup>16,95,96</sup></li> <li>• Ionic and electronic conductors based on polymer-clay nanocomposites<sup>11,95,97,98</sup></li> <li>• Carbon-clay conductive materials<sup>16,96,99,100</sup></li> <li>• Protective, anticorrosion and barrier coatings<sup>101</sup></li> </ul>   | <ul style="list-style-type: none"> <li>• Membranes for ion-exchange processes<sup>102</sup></li> <li>• Bionanocomposites for ion-detection<sup>103</sup></li> <li>• Ionic and electronic conductors based on polymer-MXene nanocomposites<sup>104,105</sup></li> <li>• Carbon-MXenes composites<sup>53,106</sup></li> <li>• Non-volatile memory devices<sup>107</sup></li> <li>• EMI shielding<sup>108,109</sup></li> <li>• High-performance corrosion inhibition<sup>110,111</sup></li> </ul>  |
| <ul style="list-style-type: none"> <li>• Electroactive and electrochemical materials</li> <li>• Energy production and storage</li> </ul>   | <ul style="list-style-type: none"> <li>• Clay-based materials as electrical insulators (dielectrics)<sup>112,113</sup></li> <li>• Electrical resistances by assembly of clays/graphite<sup>114</sup></li> <li>• Fuel-cell electrodes<sup>115</sup></li> <li>• Carbon-clay and conducting polymer-clay composites for energy storage<sup>99,116–119</sup></li> </ul>   | <ul style="list-style-type: none"> <li>• Components for supercapacitors<sup>120–122</sup></li> <li>• Use in photovoltaic devices<sup>123</sup></li> <li>• Thermoelectric power generation<sup>124</sup></li> <li>• Electrodes in Zn–air batteries, Li/Na ion batteries, Li–S batteries<sup>25,121,125–127</sup></li> </ul>  |
| <ul style="list-style-type: none"> <li>• Photoactive materials</li> </ul>  | <ul style="list-style-type: none"> <li>• Photodegradation of organic pollutants<sup>128,129</sup></li> <li>• Protection from solar and UV-radiation<sup>130</sup></li> <li>• Protection from the photodegradation of labile pesticides<sup>131</sup></li> </ul>   | <ul style="list-style-type: none"> <li>• Photocatalytic degradation of organic pollutants in water, such as dye waste<sup>132,133</sup></li> <li>• Photocatalytic fuel production, such as hydrogen H<sub>2</sub> evolution from water splitting, and CO<sub>2</sub> reduction<sup>133,134</sup></li> </ul>   |
| <ul style="list-style-type: none"> <li>• Polymer nanocomposites</li> </ul>   | <ul style="list-style-type: none"> <li>• Enhanced mechanical and thermal properties of nylon, epoxy, unsaturated polyester, engineering resins, etc.<sup>5,7,135</sup></li> <li>• Improved flame retardancy of thermoplastics and thermosets<sup>136</sup></li> <li>• Materials applied in the automotive, medical and healthcare, adhesive, building and construction sectors<sup>137–139</sup></li> <li>• Bionanocomposites as biocompatible materials<sup>139–141</sup></li> <li>• Packaging and barrier films (food, cosmetics, drugs, electronics...) <sup>99,142</sup></li> </ul>   | <ul style="list-style-type: none"> <li>• MXene-polymer nanocomposites with improved mechanical properties<sup>143,144</sup></li> <li>• MXene compounds for flame retardancy<sup>145</sup></li> <li>• NH<sub>3</sub> sensing and monitoring devices<sup>146</sup></li> <li>• MXene-based nanocomposites for piezoresistive sensors<sup>147,148</sup></li> <li>• Photothermal and photodynamic properties<sup>149,150</sup></li> <li>• Biomedical applications<sup>53,127,151–153</sup></li> <li>• Gas barrier<sup>143</sup></li> </ul>   |
| <ul style="list-style-type: none"> <li>• Food, agriculture and farming</li> </ul>  | <ul style="list-style-type: none"> <li>• Clay-organic derivatives for controlled release of agrochemical formulations<sup>154,155</sup></li> <li>• Crop-protection formulations<sup>156</sup></li> <li>• Processing of edible oils<sup>157</sup></li> <li>• Mycotoxin sequesters<sup>158</sup></li> <li>• Antifouling paints<sup>159</sup></li> </ul>   | <ul style="list-style-type: none"> <li>• MXenes in controlled pesticide release<sup>160</sup></li> <li>• MXene applications in sustainable agriculture<sup>161</sup></li> </ul>   |
| <ul style="list-style-type: none"> <li>• Pharmaceutical, biomedical and biotechnological applications</li> </ul>   | <ul style="list-style-type: none"> <li>• Clay minerals and related solids for controlled drug release<sup>162</sup></li> <li>• Clay derivatives as carriers of vaccines<sup>163</sup></li> <li>• Clay-based composites for wound healing and hemostatic applications<sup>164,165</sup></li> <li>• Clay derivatives for tissue engineering<sup>139</sup></li> <li>• Clay-based bionanocomposites for non-viral gene transfection and cancer treatment</li> </ul>   | <ul style="list-style-type: none"> <li>• MXene nanocomposites for controlled drug delivery<sup>166,167</sup></li> <li>• MXene-based nanoarchitectures for wound healing and hemostatic applications<sup>53,168</sup></li> <li>• MXene nanostructures for cancer therapy<sup>85,169,170</sup></li> <li>• Biofunctionalized MXenes for cancer detection<sup>171</sup></li> <li>• MXene polymeric composites for tissue engineering<sup>172</sup></li> </ul>   |





irradiation, giving rise to high-viscosity clay hydrogels that can be used to stabilize many diverse nanocomposites and nanoparticles, resulting in functional nano/micro-architected solids.<sup>63</sup> In turn, MXenes are produced as colloids after etching of the “A” elements from the MAX phase leading to the  $M_{n+1}X_nT_x$  compounds in water dispersion. Unlike clay minerals, these colloidal phases of MXenes are altered over time due to oxidation processes mainly attributed to their reaction with water molecules. The nature of the atmosphere (inert or oxygen-containing) adopted for their storage is an important factor in the chemical evolution of MXene flakes formed in aqueous media. For example,  $Ti_3C_2T_x$  prepared by Al etching in  $Ti_3AlC_2$  in aqueous dispersion is decomposed to anatase after hours or days depending on the nature of the atmosphere in which it is placed.<sup>64</sup> Dispersions in anhydrous solvents even in the presence of  $O_2$  preserve these MXenes against decomposition.<sup>64</sup> In contrast, the colloids generated by the dispersion of clays are very stable and do not undergo appreciable alteration due to their prolonged contact with water and exposure to the atmosphere, even with strong variations of the ambient temperature. The chemical alterations of clay minerals can only take place in the presence of aggressive acidic or basic media and high temperatures. Clay modifications occur naturally through geochemistry in the Earth, generally taking place under hydrothermal conditions that lead to mineralogical, chemical, and textural changes in clays, affected by temperature and the chemical environment, and always over very long periods of time.<sup>65</sup>

Layered materials, and particularly clay minerals as well as the composites derived from them, have been extensively investigated from the point of view of molecular modeling and solid simulations. According to Cygan *et al.*<sup>66</sup> computational chemistry techniques based on classical force field and quantum chemistry methods that are commonly employed to evaluate electronic structures offer a practical, very useful and affordable approach to evaluate the structure and dynamics of 2D solids at the atomic scale. Molecular dynamics (MD), Monte Carlo (MC) techniques and quantum methods could provide accurate models for computational studies of layered materials.<sup>66</sup> Similar computational studies on MXenes appear very useful in determining their structure–properties relationships. In particular, aspects related to atomic structure, the nature and role of terminal groups, as well as surface chemistry and electronic structural features offer the most important atomistic insights.<sup>67</sup> Computational tools are of particular interest to study more complex materials derived from MXenes, such as artificial nacre prepared by assembling MXenes and polymers arranged as nanocomposites.<sup>68</sup>

### 3. Clay intercalation vs. MXene intercalation: towards nanoarchitected functional materials

Both 2D materials, clays and MXenes, have the ability to intercalate diverse organic and inorganic compounds acceding into

their intracrystalline nanospaces following ion-exchange processes and other mechanisms. Clays and MXenes integrate in their structure nanolayers negatively charged with compensating cations in the interlayer space. The first well-defined organic–inorganic hybrid materials on record were developed by the intercalation of alkylammonium cations into smectites such as montmorillonite and related phyllosilicates (*e.g.* vermiculites) *via* cation exchange reactions.<sup>173–175</sup> In fact, the interlayer cations present in smectites (exchangeable cations) can be replaced by many positively charged inorganic or organic compounds in aqueous solution. In addition to ion-exchange process, the interlayer insertion can be controlled by diverse mechanisms such as van der Waals forces, hydrogen bonding and water bridges, electrostatic bonds, ion–dipole and coordination, proton and electron transfer, and eventually by covalent bonding (*i.e.* grafting reactions).<sup>176,177</sup> It can be postulated in a first approximation that MXene carbonitrides could also interact with compounds of a very different nature following processes similar to clays.

Fig. 4 shows a comparison between clays and MXenes regarding their ability to intercalate neutral molecules such as  $H_2O$ ,  $N_2H_2$ , DMSO, DMF, metal and organic cations including bulky polyhydroxy cations such as  $Al_{13}^{7+}$  (“Al13” Keggin-cage, *vide infra*) and surfactants (*e.g.* cetyltrimethylammonium bromide, CTAB), polymers leading to polymer–clay nanocomposites, bionanocomposites, 3D silica networks, and small NPs (*e.g.*, carbon nanomaterials), in some cases assisted by intercalation–delamination processes.

For instance, similarly to smectite clays,  $Ti_3C_2T_x$  MXenes lead to the spontaneous intercalation of neutral organic molecules such as hydrazine hydrate, *N*-methylformamide (NMF), DMF, DMSO, urea, *etc.*<sup>39,178,179</sup> Cations of diverse nature, such as  $Li^+$ ,  $Na^+$ ,  $K^+$ ,  $NH_4^+$ ,  $Mg^{2+}$  and  $Al^{3+}$ , could be easily incorporated to the MXenes following ion-exchanging processes.<sup>120</sup> The accessibility to the interlayer space depends on the experimental conditions adopted during the etching of the MAX phase (Fig. 5). However, when the etching process was carried out in the absence of lithium salts the ion-exchanges were disfavored. In fact, the presence of  $Li^+$  ions in the interlamellar space attained by HF/LiCl treatments of the MAX phase facilitates the easy exchange by alkali and alkaline earth cations (*e.g.*,  $Na^+$ ,  $K^+$ ,  $Rb^+$ ,  $Mg^{2+}$  and  $Ca^{2+}$ ). As occurs in clay minerals, the basal spacing values of these 2D carbonitrides varies with the nature of the interlamellar cation as well as the relative humidity.

Compared with MXenes, 2D charged clay minerals (*e.g.* smectites and vermiculites) show relatively weak interactions between consecutive structural nanolayers. In fact, MXenes have a higher surface charge density than lamellar clays, so that to promote their exfoliation these carbides may require the application of shear forces, following a process similar to that proposed by Ma and Sasaki for transition metal oxides and hydroxides.<sup>9</sup>

#### 3.1. Pillared clays and MXenes

Intercalations based on ion-exchange mechanisms occurring in 2:1 charged silicates (*e.g.* smectites and vermiculite clay




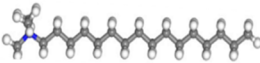

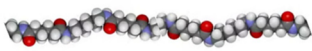

| Examples of intercalation  | Clays   | MXenes   |
|--|---|--|
| <b>Metal cations</b>      | Metal & complexed cations, "Al13", ..   | Li <sup>+</sup> , Na <sup>+</sup> , .. K <sup>+</sup> Ca <sup>2+</sup> , Mg <sup>2+</sup> , "Al13", .. |
| <b>Organic cations</b>    | Onium ions (alkylammonium, etc)   | Alkylammonium ions<br>Ionic liquids  |
| <b>Neutral molecules</b>  | H <sub>2</sub> O, DMSO, DMF, urea<br>alcohols, amines,<br>carbohydrates                               | H <sub>2</sub> O, DMSO, DMF, urea,<br>amines, ..   |
| <b>Polymers</b>           | Nylon, PEO, PVA, PANI,<br>epoxies, PVP, organo-<br>silanes, biopolymers..                             | Nylon, PEO, PVA, PANI,<br>organosilanes,<br>biopolymers  |
| <b>Nanoparticles</b>      | C-nanoparticles, SiO <sub>2</sub> ,<br>TiO <sub>2</sub> , Al <sub>2</sub> O <sub>3</sub> , Ag, Au, .. | C-nanoparticles, MOF,<br>SiO <sub>2</sub> , montmorillonite..  |

Fig. 4 Scheme comparing the intercalation capacity of various chemical species in the interlayer space of clay minerals and MXene 2D solids, leading to their corresponding derivatives.

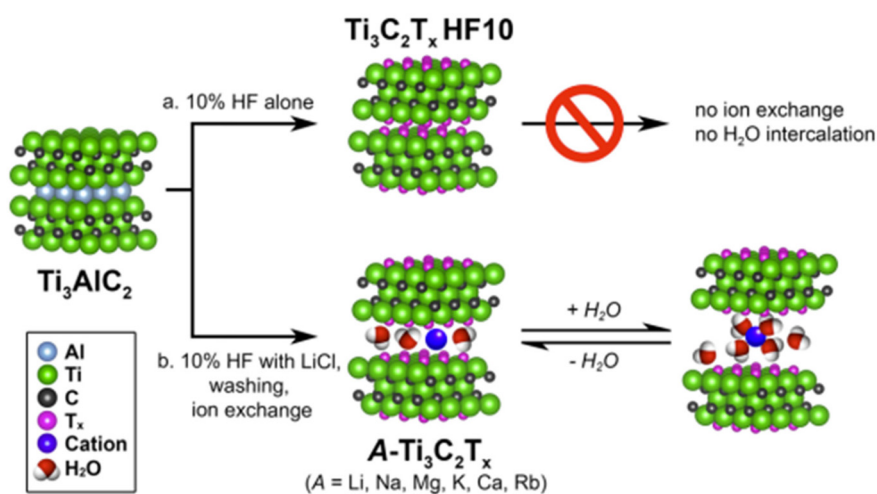


Fig. 5 Scheme showing the preparation of MXenes from the  $\text{Ti}_3\text{AlC}_2$  MAX phase etched with (a) 10% HF alone (which does not intercalate cations and water molecules), and (b) 10% HF in the presence of LiCl (leading to  $\text{A-Ti}_3\text{C}_2\text{T}_x$  materials possessing ion-exchange and reversible  $\text{H}_2\text{O}$  adsorption properties in the interlayer space). Reprinted with permission from Ghidui *et al.*, *Chem. Mater.*, 2016, 28(10), 3507–3514. Copyright 2016 American Chemical Society.

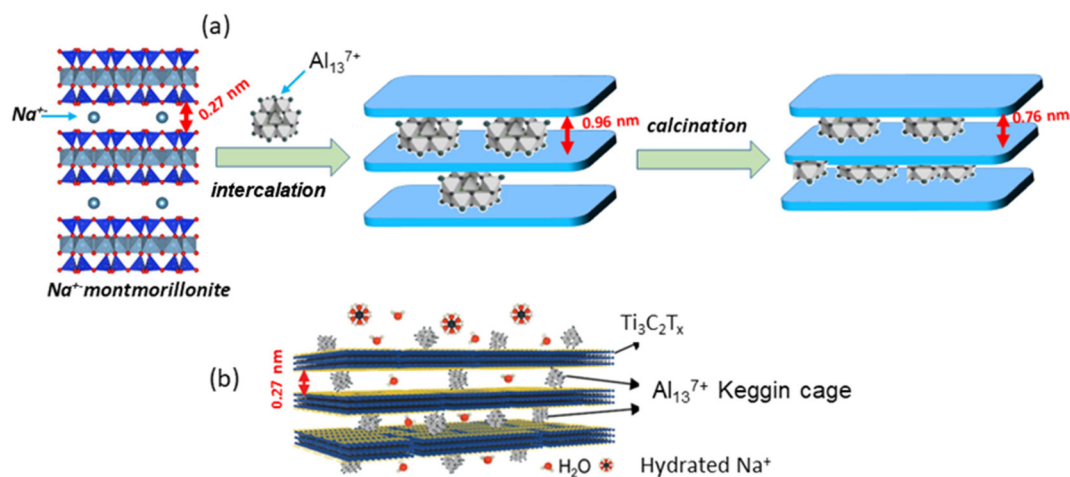
minerals) may involve bulky positively charged inorganic species such as highly charged cage-like polyhydroxy cations, *e.g.*  $[\text{Al}_{13}\text{O}_4(\text{OH})_{24}(\text{H}_2\text{O})_{12}]^{7+}$ , the Keggin cage abbreviated as  $\text{Al}_{13}^{7+}$  or even "Al13". These polycations have been used to prepare the so-called "pillared clays" intensely studied in the last 40 years.<sup>21,70,180–183</sup> This type of bulky cation produces an expansion between the layers of the 2D solid of approximately 1 nm, in which after a calcination step, typically by heating at 300–500 °C, the Al13 is transformed into alumina pillars that bonded to the silicate layers. The resulting pillared clay materials are provided with a large specific surface area associated with a permanent micro- and meso-porosity and showing molecular sieving functions. The reproducible generation of pillared clays in large quantities regarding various industrial

applications, particularly adsorption and heterogeneous catalysis, was the objective of big projects developed in the past decades.<sup>184</sup>

The interlayer insertion of inorganic clusters or nanoparticles including  $\text{Al}_{13}^{7+}$  polycations is highly interesting to prepare functional nanoarchitectures useful as efficient membranes, heterogeneous catalysts and energy storage components.<sup>37,185</sup>

Following a similar way to that reported several decades ago for clay minerals (Fig. 6),  $\text{Al}_{13}^{7+}$  polycations can be strongly and homogeneously bonded onto the surface of the  $\text{Ti}_3\text{C}_2\text{T}_x$  nanosheets through electrostatic mechanisms showing variable *d*-spacing values (0.27–1.12 nm) depending on the adopted experimental conditions and the nature of the initial





**Fig. 6** Schematic representation of the preparation of Al<sub>13</sub> pillared clays based on homoionic (Na<sup>+</sup>) montmorillonite (a) with *d*-spacing values from the reference,<sup>181</sup> and the structural arrangement showing Al<sub>13</sub>-Ti<sub>3</sub>C<sub>2</sub>T<sub>x</sub> pillared MXene (b) formed by the assembly of the Al<sub>13</sub><sup>7+</sup> polycations with Ti<sub>3</sub>C<sub>2</sub>T<sub>x</sub> nanosheets in a colloidal solution (reprinted with permission from Zhu *et al.*, *ACS Nano*, 2020, 14(11), 15306–15316. Copyright 2020 American Chemical Society).

mixture of components.<sup>37,185</sup> In this way, by tuning the preparation conditions of the Al<sub>13</sub>-MXenes, 2D arrangements with basal spacings that can be adjusted over a wide range of high-precision *d*-spacing values (with a scale accuracy of 0.1 nm) are achieved. Thus, the properties of the pillared Ti<sub>3</sub>C<sub>2</sub>T<sub>x</sub>-based MXenes are suitable for the fabrication of membranes with marked selectivity towards cations depending on their valence and showing wonderful performance in monovalent ion rejection.<sup>37,185</sup> The resulting material derived from the Ti<sub>3</sub>C<sub>2</sub>T<sub>x</sub> MXene was named “Al<sub>13</sub>-Ti<sub>3</sub>C<sub>2</sub>T<sub>x</sub> clay”, but we must clarify that it differs significantly from typical Al<sub>13</sub> pillared clays. In fact, in the latter, Al<sub>13</sub><sup>7+</sup> polycations are transformed into alumina pillars by calcination at temperatures above 300 °C, which, to our knowledge, has not been applied in Al<sub>13</sub>-MXenes to date. These thermal treatments can be carried out both by conventional heating and by microwave irradiation<sup>181</sup> with the aim to consolidate the Al<sub>13</sub> pillars which, in this way, are transformed into protonated alumina pillars useful for acid catalysis processes.

Silica-pillared clays have been prepared at the end of the last century by diverse intercalation approaches using smectites like montmorillonite and diverse pillaring precursors, such as tris(acetylacetonato)-silicon(IV) cations, *i.e.* Si(acac)<sub>3</sub><sup>+</sup> (ref. 186) and alkoxy silanes,<sup>187,188</sup> allowing a permanent separation of the silicate nanosheets and enlarging the specific surface area of the clay mineral. The attempts to intercalate the hydrolyzed silica sol in montmorillonite by direct treatments were also reported by Moini and Pinnavaia,<sup>189</sup> obtaining silica-clay solids possessing a relatively large surface area (250–460 m<sup>2</sup> g<sup>-1</sup>). According to the XRD data, these latter materials do not exhibit regular intercalation phases as is typically observed in other pillared clay materials.

Letaïef and Ruiz-Hitzky described a new family of silica-clay materials that could be assimilated to inorganic–inorganic

nanocomposites, as they consist of silicate nanosheets from delaminated clays dispersed in silica matrices (Fig. 7a).<sup>190</sup> These silica-clay porous materials are produced through sol-gel processes using silicon alkoxides as precursors that react with smectites and vermiculites expanded by the previous intercalation of CTAB and other alkylammonium species.<sup>21,191</sup>

Like clay minerals, MXenes can also be pillared with silica and even delaminated by inclusion in silica matrices. In this way, SiO<sub>2</sub>-pillared Ti<sub>3</sub>C<sub>2</sub>T<sub>x</sub> MXenes have been recently synthesized in a first step by the co-intercalation of amines such as dodecyl- and octyl-amine in the presence of silicon alkoxides used as a silica precursor (*e.g.*, tetraethyl orthosilicate (TEOS)). In a second step the resulting materials are calcined by heating under an argon atmosphere at temperatures ranging from 300 to 500 °C (Fig. 7b).<sup>192</sup> A shift to lower angles is observed in the XRD patterns, particularly the (002) diffraction peak, indicating the increase of the interlayer spacing in the MXene reaching a maximum value of 3.2 nm. The resulting open structure due to the pillaring effect shows an extraordinary increase of the specific surface area showing values of 235 m<sup>2</sup> g<sup>-1</sup>, which is twice the maximum surface area achieved by MXene-based materials.<sup>192</sup> Interestingly, the presence of electroactive components in MXenes, unlike clays, can be used in the development of electrode materials for electrochemical devices. SiO<sub>2</sub>-pillared Ti<sub>3</sub>C<sub>2</sub>T<sub>x</sub> materials have been successfully used as electrodes for Na<sup>+</sup>-ion batteries, showing superior capacity, rate capability, and stability compared with those of pillar-free materials.<sup>192</sup>

The original works based on clays could be taken nowadays as an example for future developments of new MXene-based pillar materials. Thus, other precursor agents for pillar formation, already applied in the preparation of silica-clays, such as Si(acac)<sub>3</sub><sup>+</sup> as proposed by Endo *et al.*<sup>186</sup> or such as mixtures of SiO<sub>2</sub> and metal-oxides as investigated by Han *et al.*,<sup>188</sup> could



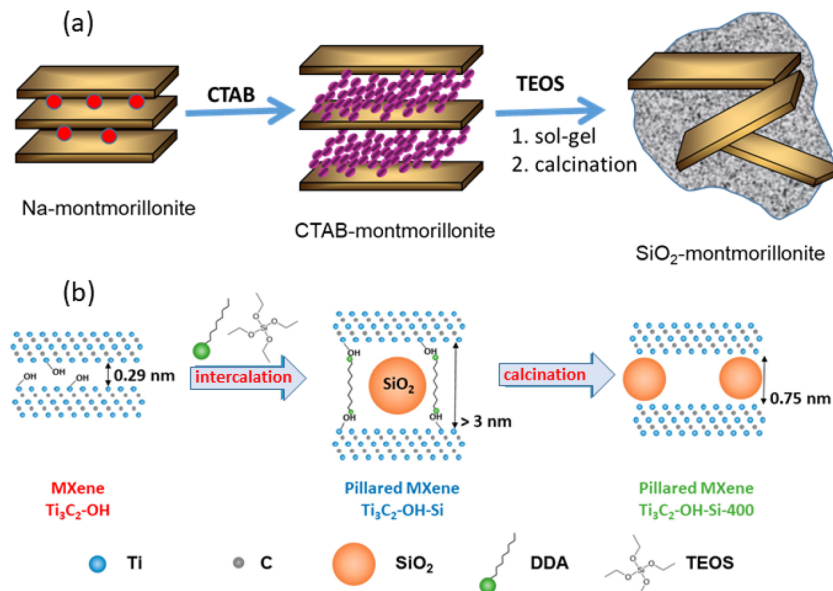


Fig. 7 Scheme showing: (a) the assembly of silica to delaminated 2:1 charged clay minerals through previous intercalation of CTAB and further reaction with an alkoxysilane (e.g., TEOS), as reported by Letaief and Ruiz-Hitzky,<sup>190</sup> and (b) pillaring of Ti<sub>3</sub>C<sub>2</sub>T<sub>x</sub>-MXene by silica introduced by the intercalation of TEOS in the presence of alkylammonium species (figure from ref. 192 licensed under CC-BY).

be potentially adopted for the preparation of new silica-MXene pillared solids. In addition, the insertion of pillars of different compositions, including for instance Ti, Zr, Zn and Fe oxides, have been developed in layered clays,<sup>193–197</sup> representing potential interest for the development of functional MXene-based pillared materials. In this context, pillars such as SnS with an electroactive response have recently been assembled to MXenes. The resulting solids have been successfully applied to the fabrication of Li<sup>+</sup>-battery electrodes with an improved capacity in successive cycles, which has been attributed to the “pillar effect” of the SnS/Ti<sub>3</sub>C<sub>2</sub>T<sub>x</sub> pillared MXenes.<sup>198</sup>

Qin *et al.* have recently described the fabrication of silicate-based nanocomposites incorporating MXenes prepared by the ultrasonic treatment of clay dispersions in the presence of MXene.<sup>199</sup> To explain the observed protective effect of clay against spontaneous MXene oxidation, a mechanism of Ti<sub>3</sub>C<sub>2</sub>T<sub>x</sub> MXene intercalation within the montmorillonite layers has been proposed by this author and collaborators. However, it is difficult to explain such a structural organization because both 2D solids present negatively charged surfaces, pointing to their electrical charge incompatibility as both components exhibit negatively charged surfaces. Furthermore, the XRD patterns of the resulting materials do not agree with the expected increase of the basal spacing of montmorillonite by intercalated MXene nanolayers. In our opinion, the assembly of the montmorillonite clay mineral with Ti<sub>3</sub>C<sub>2</sub>T<sub>x</sub> could be tentatively explained by a steric hindrance preventing the restacking of the interpenetrating clay and MXene flakes. A comparable assembly between a 1:1 layered clay, such as kaolinite, and sepiolite fibrous clay has been also attempted by ultrasonication of the corresponding silicate dispersions.<sup>63</sup> Interestingly, the MXene-based composite materials integrate

the photothermal properties inherent in the presence of the titanium carbide, being efficiently activated by NIR laser (e.g., 808 nm) irradiation, reaching temperatures in the order of 70 °C within a few minutes. These clay-MXene materials can include Ag<sup>+</sup> ions that are reduced *in situ* to metallic Ag NP, and the resulting materials show marked and long-lasting antibacterial activity.<sup>199</sup>

Besides that, multilayer MXene-clay nanoarchitectures have been prepared by layer-by-layer (LbL) procedures leading to freestanding thin films resulting from the assembly of Ti<sub>3</sub>C<sub>2</sub> MXene, poly(vinyl alcohol) (PVA) and montmorillonite.<sup>200</sup> These nanocomposites show a very high tensile strength imparted by the clay mineral, the PVA acts as a flexible polymer binder and the MXene provides suitable performance as a lightweight EMI shielding material.

### 3.2. Clay- and MXene-based carbon nanocomposites

Although carbon (e.g. graphite) and clay minerals (e.g. kaolinite) are very different types of material, their combination by mixing both finely divided components has long been described for use as electrical resistors<sup>201</sup> or as pencil cores.<sup>96</sup> Since the 1980s, these materials have been used to prepare diverse functional carbon-clay nanocomposites by modifying their initial properties, such as the texture and the surface chemistry characteristics, paving the way for key fields of application related to energy storage,<sup>117</sup> heterogeneous catalysis,<sup>202</sup> food packaging,<sup>96</sup> sensing devices<sup>96</sup> and environmental remediation.<sup>202</sup> In these composites the presence of the clay increases the hydrophilicity introduced by the carbon moiety, allowing the incorporation of other components, for example hydrogel polymers<sup>96,203</sup> and metal nanoparticles<sup>202,204</sup> among other constituents, thus enlarging their applicability.



Two general approaches can be described for preparing carbon-clay materials (Fig. 8): (i) top-down processes, by simply and directly assembling the two individual components, and (ii) bottom-up procedures, growing the carbon on the clay surface. Top-down approaches (Fig. 8) use as starting materials small graphite particles or graphene nanoplatelets (GNP), which, by grinding<sup>205,206</sup> or by dispersion in water under high shear or ultrasonication treatments in the presence of the clay minerals, give rise to carbon-clay nanocomposites.<sup>96,207,208</sup> The role of clay minerals in their assembly with GNP and MWCNT is crucial, particularly in the case of sepiolite since it can generate high-viscosity dispersions<sup>63</sup> leading to the steric stabilization of carbon nanoparticles, preventing their rebound and maintaining the carbon-sepiolite in homogeneous dispersion for a long time (several years).<sup>208</sup> Water dispersion processes allow the incorporation of soluble or easily dispersible compounds such as hydrogels like PVA and biopolymers like chitosan, alginate or gelatin, leading to bionanocomposites that can be doped with MWCNT, enhancing their electrical conductivity while maintaining their mechanical properties.<sup>96</sup>

Concerning the bottom-up approach, Kyotani's group was the pioneer in the application of this procedure, intercalating polyacrylonitrile (PAN) as a carbon precursor in the interlayer space of montmorillonite, followed by a thermal treatment in the absence of oxygen.<sup>209–211</sup> These processes were carried out at high temperature (>1000 °C), resulting in well-crystallized graphite that remains intercalated between the clay silicate layers.<sup>209</sup> Related studies were conducted employing diverse clay minerals such as lamellar smectites and vermiculites,<sup>212,213</sup> and fibrous silicates such as sepiolite.<sup>117,213</sup> Diverse carbon precursors including PAN,<sup>214</sup> sucrose (table sugar),<sup>212,215,216</sup> biopolymers,<sup>216</sup> asphaltenes<sup>217</sup> and caramel<sup>117,213</sup> among others give rise to carbon-clay nanocomposites based on graphene-like materials supported on these silicates under treatments at temperatures much lower (450–750 °C) than those initially adopted by Kyotani, saving energy and avoiding structural alterations of the silicate fraction. The proposed mechanism to explain the generation of

graphene-like materials under these experimental conditions, for instance in the case of sucrose-sepiolite (Fig. 8) as starting components, points to the role of the intrinsic porosity of the silicate that could retain volatile intermediate compounds (*e.g.* furfuraldehydes) generated during the pyrolysis of the carbohydrate, facilitating their subsequent polycondensation towards graphene-like compounds (*unpublished results*). The resulting conductive composites exhibit a reduced conductivity compared with graphene materials but they can merit application as active components of electrochemical devices, including batteries, supercapacitors and sensors<sup>100</sup> and pulsed electric field (PEF) processes for “cold sterilization”, of great interest in food packaging.<sup>218</sup>

The combination of intrinsically insulating solids such as clays and graphene materials results in a decrease of electronic conductivity whereas conductive MXenes could enhance the resulting conductivity. In this way, replacing clay by MXenes in carbon-clay materials by applying top-down and bottom-up methodologies, it is expected to obtain higher conducting materials. In this way, MXene-carbon composites can be prepared from polymers such as PAN<sup>219</sup> and block copolymer P123/melamine-formaldehyde resin,<sup>122</sup> or from carbon gases such as ethene,<sup>220</sup> obtaining carbon nanofibers, mesoporous carbons and CNT, respectively, assembled on the MXenes. As well, these composites have been obtained from the intimate mixture of the carbon particles and the MXenes, as a top-down process, by dispersion in the liquid phase of graphene<sup>221,222</sup> or CNT<sup>223</sup> and MXenes, or by direct grinding of these components.<sup>224</sup> The synergetic effect of carbon and MXenes is boosted and improves the electronic properties of these materials, presenting them as excellent candidates as electrodes in electrochemical devices, for instance supercapacitors.<sup>219,222</sup>

In addition, carbon-MXene composites show attractive surface properties with a potential impact as new materials for environmental remediation. For instance, delaminated  $Ti_3C_2T_x$  MXenes could be assembled to porous carbon microspheres, impeding their restacking and producing solids of elevated specific surface area (>800 m<sup>2</sup> g<sup>-1</sup>) acting as superadsorbents

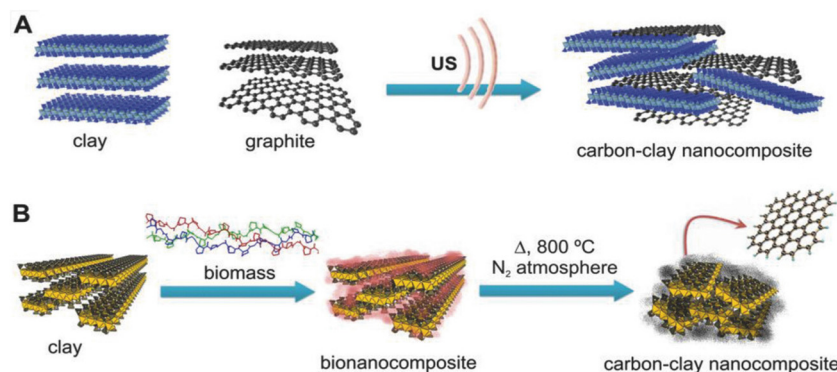


Fig. 8 Scheme showing bottom-up (A) and top-down and bottom-up (B) procedures for the preparation of carbon-clay nanocomposites. Figure from Darder *et al.*, *Adv. Funct. Mater.*, 2018, 28, 1704323, Wiley.



of pollutants.<sup>225</sup> It can be assumed that the incipient results shown by these emerging MXene-carbon composites have a promising future for the preparation of new advanced systems of interest in critical fields of application. The key is the combination of the metallic character with electrical conductivity, porosity and surface properties with high adsorption capacity, together with their hydrophilic character allowing stable colloidal dispersions and co-assembly with many diverse components of polar nature.

### 3.3. Clay- and MXene-based polymer nanocomposites

In the world of organic–inorganic hybrid materials, the discovery of polymer-clay nanocomposites by Fukushima and other Toyota researchers, by the synthesis of an intercalated compound of montmorillonite and 6-polyamide,<sup>226,227</sup> had an enormous impact from the fundamental and application points of view. Thus, the preparation in this way of polymer-clay nanocomposites, a new class of composites where the dispersed phase (*i.e.* the silicate) is constituted by particles that have at least one of their dimensions in the nanoscale, represents an important advancement in the composite materials field.<sup>177,228,229</sup> These revolutionary hybrid materials are achieved by a delamination of the silicate in the polymer matrix, allowing extraordinary enhancement of the mechanical properties with a very low content of reinforcing clay (<5% w/w). In the example proposed by Toyota in the 1980s regarding the 6-polyamide/montmorillonite, an increase of *ca.* 70% in the Young modulus and 126% in the flexural modulus was reached by incorporation of *ca.* 4% w/w of clay over the polyamide in comparison with the pure polymer.

Analogous systems related to polymer-clay nanocomposites were prepared using various 2D solids such as layered transition metal oxides (*e.g.* V<sub>2</sub>O<sub>5</sub> xerogel), layered phosphates (*e.g.* Zr-phosphate), transition metal chalcogenides (*e.g.* MoS<sub>2</sub>) and graphene-based solids. In this context, more recently, MXenes have been used as the disperse phase of diverse polymer matrices.<sup>230</sup> In a similar way to clay minerals, Ti<sub>3</sub>C<sub>2</sub>T<sub>x</sub> nanosheets have been successfully dispersed in polyamide-6 by  $\epsilon$ -caprolactam intercalation followed by reaction with 12-aminolauric acid.<sup>231</sup> In addition to these hybrid materials and exactly as in the case of clay minerals, other polymer-MXene nanocomposites have been prepared with polymeric matrices of a very diverse nature, such as poly(acrylic acid) (PAA), of interest as structural materials, conductive polymers, such as PEO, polyaniline (PANI) and polypyrrole (PPy), as well as biopolymers such as chitosan and nanocellulose. Conducting polymers such as PEO and PANI were pioneering intercalation compounds using layered clay minerals.<sup>11,15,232–235</sup> The resulting clay-polymer nanocomposites exhibit electronic conductivity when PANI or PPy is the intercalated polymer<sup>168</sup> and ionic conductivity when they incorporated PEO that facilitates the ion-mobility of interlayer cations.<sup>236–238</sup> These nanoarchitectures have properties of interest in electrical and electrochemical devices, but the presence of clay components with insulating characteristics

reduces their application capacity where ideally the conductivity should have outstanding values.

Semiconducting 2D solids, such as certain metal oxides and dichalcogenides of transition metals (*e.g.*, V<sub>2</sub>O<sub>5</sub> xerogel and MoS<sub>2</sub>) used as hosts for the intercalation of conducting polymers, show an enhancement of the electronic conductivity, demonstrating mixed ionic-electronic conductivity when PEO is incorporated in these systems.<sup>3,239–241</sup> The recent use of MXenes provided with elevated electrical conductivity represents an attractive way to improve the properties of the intercalated electroactive polymers, leading to new functional organic–inorganic nanoarchitectures dealing with applications in diverse devices.<sup>242</sup>

The intercalation of PEO in smectite clays gives rise to materials showing anisotropic ion-conductivity, typically in the order of 10<sup>-7</sup>–10<sup>-4</sup> S cm<sup>-1</sup> in the layer plane, which is much higher than the value measured in the perpendicular direction.<sup>11,233</sup> MXene-PEO nanocomposites prepared by the incorporation of lithium bis(trifluoromethanesulfonyl)imide (LiTFSI), a lithium salt, show low ionic conductivity (around 10<sup>-7</sup> S cm<sup>-1</sup>),<sup>243</sup> and the 2D MXene arranged as disorganized platelets with a random distribution of delaminated carbide layers (Fig. 9). The electronic conductivity of PEO-MXene nanocomposites ascribed to the MXene component is very low (in the order of 10<sup>-10</sup> S cm<sup>-1</sup>), probably due to the presence of insulating PEO chains involving a structural organization unable to form a favorable percolation pathway.

### 3.4. Biohybrid nanoarchitectonics based on clays and MXenes

Biohybrid materials result from the nanoscale combination of whole living cells or some of their fragments and inorganic components, giving rise to complex systems that can be endowed with extraordinary bioactivity.<sup>176,244</sup> Among these types of material, bionanocomposites have been defined as biohybrids that involve the assembly of natural polymers with inorganic nanoparticles,<sup>245</sup> including clay minerals and more recently MXenes interacting at the nanoscale. The diverse processing strategies have been reviewed by Ojijo and Ray, discussing the methods used in the preparation of bionanocomposites.<sup>246</sup> Bionanocomposites based on clay minerals have been intensively studied to produce hybrid materials whose

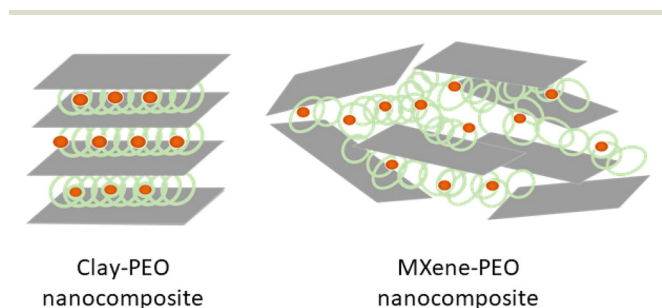


Fig. 9 Structural arrangements of clay-PEO based on montmorillonite layered clay mineral, described by Ruiz-Hitzky and Aranda,<sup>233</sup> and MXene-PEO based on Ti<sub>3</sub>C<sub>2</sub>T<sub>x</sub>, described by Pan *et al.*<sup>243</sup>



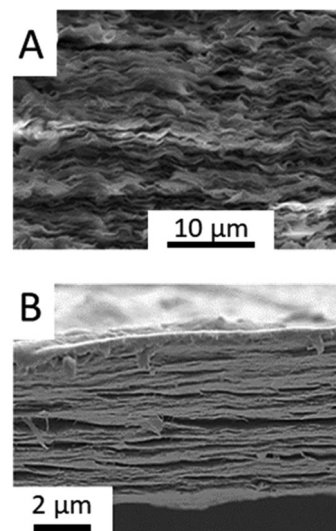
properties are defined both by the nature of the inorganic part and by the properties of the biopolymers involved.<sup>129,140,247</sup> These materials are attracting an increase of interest since the participation of natural polymers can offer additional properties to the clay components, resulting in sustainable composite materials that also show biodegradability/biocompatibility, thus widening the field of their applications. The main envisaged applications of clay-based bionanocomposites are aimed at bioplastics, packaging, sensors, tissue engineering and environmental protection. Typical clay minerals used as the inorganic component are montmorillonite, halloysite, sepiolite, palygorskite, kaolinite, hectorite (LAPONITE®) and vermiculite. The 2D charged phyllosilicates such as montmorillonite, hectorite and vermiculite can act as a host for the intercalation of biopolymers or to assemble them through delamination processes, whereas nanotubular halloysite and nanofibrous sepiolite interact through their external surfaces.<sup>248,249</sup> With regard to the biopolymers involved, most are polysaccharides such as chitosan, alginate, starch cellulose and chitosan and, to a lesser extent, some proteins such as gelatin and zein and nucleic acids such as DNA and RNA, as well as certain biocompounds produced by microorganisms (e.g., polylactic acid, PLA).<sup>248,249</sup>

The chitosan-montmorillonite bionanocomposite is produced by intercalation involving ion-exchange processes that displace the interlayer cations of the clay because the involved chitosan is present in its protonated form. These bionanocomposites show a well-ordered structural arrangement together with anion exchange properties<sup>12</sup> that allow the development of ion-selective sensors specially towards monovalent anions and particularly towards nitrate species, whose recognition could be controlled by automatic systems using artificial intelligence.<sup>94,250</sup> Sepiolite-chitosan also exhibits ion-selectivity, the mechanical properties of the resulting bionanocomposite being enhanced with respect to the starting biopolymer.<sup>93,247,251</sup>

Illustrative examples of recently reported clay-based bionanocomposites include biopolymers such as synthetic nanocellulose and nucleic acids (DNA, etc.). The preparation of artificial nacre by the intercalation of organic compounds in clay minerals was first reported by Kotov's team<sup>252</sup> and more recently studied by Sung *et al.* (Fig. 10A).<sup>253</sup> Nanocellulose-clay composites represent an important group of bionanohybrids with excellent mechanical properties that can be also involved in the synthesis of artificial nacre by assembling to MXenes (Fig. 10B).<sup>143</sup>

Clay-based biohybrids incorporating nanocellulose have been recently used for the preparation of multifunctional nanoarchitectures by the further assembly of nanocomponents such as carbon nanomaterials (e.g., MWCNT), magnetic nanoparticles (e.g., Fe<sub>3</sub>O<sub>4</sub>) and nanoparticulate semiconductors (e.g., TiO<sub>2</sub>, ZnO).<sup>254</sup>

As first stated by Choy and collaborators,<sup>6</sup> clay-DNA bionanocomposites are of great interest in biomedicine for gene transfection as well as in future advanced information storage. Sepiolite-DNA has recently been used as an



**Fig. 10** SEM images of bionanocomposite films showing the cross-section of films consisting of (A) clay-based artificial nacre prepared by the intercalation of 11-(methacryloyloxy)undecyltrimethylammonium cations in sodium montmorillonite clay, reprinted with permission from Sung *et al.*, *ACS Omega*, 2017, 2(11), 8475–8482. Copyright 2017 American Chemical Society; and (B) the cross-section of a film of artificial nacre based on MXene-nanocellulose bionanocomposites, reprinted from *Carbohydrate Polymers*, 299, Tang *et al.*, Nacre-inspired biodegradable nanocellulose/MXene/AgNPs films with high strength and superior gas barrier properties, 120204, Copyright (2023), with permission from Elsevier.

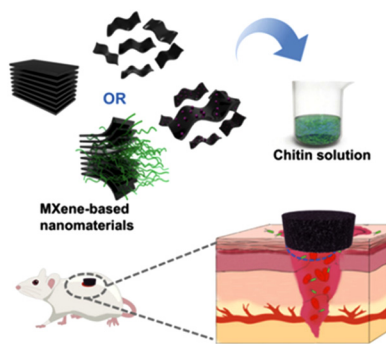
efficient nanoplatform for DNA transfer into mammalian cells.<sup>255,256</sup>

MXenes have been also assembled to biopolymers mainly by delamination/re-stacking processes allowing the preparation of transparent conductive films of functional bionanocomposites, pointing to their applications for supercapacitors, Li-ion batteries, EMI shielding, sensors, electrocatalysis, biomedicine and environmental remediation among other fields of interest.<sup>257</sup> For instance, chitosan and other polysaccharides assembled to MXenes (e.g. Ti<sub>3</sub>C<sub>2</sub>T<sub>x</sub>) give multifunctional biohybrid nanoarchitectures tested in diverse biomedical applications.<sup>258</sup>

For certain applications, bionanocomposites could be prepared as foams or sponges by gas foaming or conventional freeze-drying processes involving hydrophilic biopolymers, such as polysaccharides (e.g., cellulose and chitosan) or proteins (e.g., gelatin), which disperse easily in water together with the inorganic counterpart.<sup>259</sup>

As a selected comparative example of clay minerals and MXene nanoarchitectures, chitosan-clay nanocomposites based on rectorite layered silicate have been successfully applied as efficient hemostatic agents (*in vitro* porcine skin model), confirming that viscous injectable clay/chitosan nanocomposites act as a facile and sustainable biomaterial for skin hemostasis, as they can stably adhere to skin and impede bleeding.<sup>260</sup> Chitin-MXene composites based on Ti<sub>3</sub>C<sub>2</sub>T<sub>x</sub> have been prepared as sponges showing excellent behavior for





**Fig. 11** Bionanocomposites as hemostatic agents based on chitin assembled to MXenes. Adapted from Li *et al.*, MXene-enhanced Chitin Composite Sponges with Antibacterial and Hemostatic Activity for Wound Healing, *Adv. Healthcare Mater.*, 2022, 2102367, Wiley.

hemostasis as well as antibacterial infected wound healing (Fig. 11).<sup>53</sup> It is here assumed that the photothermal effect inherent in MXene incorporated into these bionanocomposites efficiently contributes to their antibacterial activity. MXenes (*e.g.*,  $\text{Ti}_3\text{C}_2$ ) are biocompatible nanosheets, showing a high photothermal-conversion efficiency allowing *in vitro/in vivo* photothermal ablation of tumors, representing a great potential for diverse biomedical applications and particularly in cancer therapy. For instance, Lin *et al.* reported on MXene materials presenting high absorption in the NIR region for highly effective photothermal ablation of tumors in mouse models *in vivo*.<sup>170</sup>

Other uses of MXene bionanoarchitectures deal with a broad field related to health, from theranostics<sup>261</sup> to piezoelectric sensors for the real-time monitoring of certain human activities.<sup>148</sup>

## 4. Concluding remarks

Why should clay scientists be interested in MXenes? Why should experts on MXenes be interested in clay minerals? The answer to these questions could be found above as we have shown in this critical review, a comparison between both types of solid, which share essential characteristics such as structural features and certain physical and chemical properties, particularly those related to the nature of their surface and their rheological behaviors, as well as their metallic or insulating character. It should be noted that the electrical conductivity properties are decisive in finding applications, which can be much wider in MXenes with high conductivity compared with clays, which are insulators or ionic conductors with very low electrical conductivity values.

Among the common properties of both types of solid, MXenes and 2D clay minerals belonging to the smectites and vermiculites show intercalation properties as well as the ability towards exfoliation or delamination into single layers. These characteristics allow the development of new functional nanoarchitectures prepared from their assembly with diverse

entities such as nanoparticles, biopolymers, or even microorganisms such as viral particles and living cells.

A less studied aspect of MXenes refers to their rheological properties, which have been widely studied in clays, especially regarding the microfibrillar sepiolite. This behavior can represent an example of inspiration for further rheological studies involving the MXenes.

The structural analogies between clays and MXenes lead to exceptional common surface and rheological properties and thus enable advanced applications in various fields, such as powerful selective membranes, adsorbents and absorbents, heterogeneous catalysts and insulating materials used in building sector among other uses, which could be applicable to both types of 2D solid. The additional characteristic of the MXenes in terms of their electronic conductivity allows the inclusion of important further applications<sup>249</sup> such as energy production and storage,<sup>25,106,120</sup> sensor devices,<sup>103</sup> “cold sterilization” based on PEF processes,<sup>219</sup> and bioactive materials of interest in diverse biomedical applications.<sup>53,167,168</sup>

In addition, hollow nanotubular halloysite clay presents a molecular storage capacity allowing loading with diverse functional agents, which can also serve as inspiration for new applications of MXenes or partially etched MAX carbides. The tendency of MXene flakes to roll up, creating equivalent nanotubular conformations, should be considered. On the other hand, the ability to intercalate and delaminate forming nanosheet dispersions, already well known for  $\text{V}_2\text{O}_5$  xerogel and other 2D solids such as transition metal oxides and chalcogenides (*e.g.*,  $\text{MoS}_2$ ) showing electrical conductivity typical of semiconductors, could be profitable for the equivalent studies of MXenes.

Moreover, it should also be considered that computational chemistry studies not only appear to be of enormous theoretical interest in predicting and determining the structural characteristics and derived properties of 2D-based nanoarchitectures resulting from both clay minerals and MXenes, but also that these studies represent a powerful tool for the rational advancement of new applications of these emerging materials.

Finally, it could be also concluded that the terminology recently observed in publications on MXenes does not seem fully accurate regarding the use of the term “clay” to refer to these carbides/carbonitrides. However, the MXene topic can be considered as an inspiring subject for clay scientists and, in the same way, the studies related to clay minerals are of great interest to researchers working on MXenes. In fact, it would be considered that important characteristics of these transition-metal carbides and nitrides are closely related to other 2D solids showing the ability to intercalate, exfoliate and form colloidal systems in a similar way to clay minerals. Therefore, the deep knowledge so widely achieved in the science and technology of clays in recent decades may have great potential to contribute to the rapidly advancing research on MXenes and related materials currently underway.





## Author contributions

E. R-H: conceptualization, supervision, writing – original draft and review & editing; C. R-G: visualization, writing – original draft and review & editing.

## Conflicts of interest

There are no conflicts to declare.

## Acknowledgements

We gratefully acknowledge financial support from the PID2019-105479RB-I00 (MCIN/AEI/10.13039/501100011033) project. We acknowledge Prof. M. Cambor for assistance in the graphics of clays and MXenes structural models.

## References

- R. Schöllhorn, *Phys. B + C*, 1980, **99**, 89–99.
- R. Schöllhorn, *Chem. Mater.*, 1996, **8**, 1747–1757.
- E. Ruiz-Hitzky, R. Jimenez, B. Casal, V. Manriquez, A. S. Ana and G. Gonzalez, *Adv. Mater.*, 1993, **5**, 738–741.
- G. Alberti, M. Casciola and U. Costantino, *J. Colloid Interface Sci.*, 1985, **107**, 256–263.
- S. Sinha Ray and M. Okamoto, *Prog. Polym. Sci.*, 2003, **28**, 1539–1641.
- J. Choy, S. Choi, J. Oh and T. Park, *Appl. Clay Sci.*, 2007, **36**, 122–132.
- A. Usuki, Y. Kojima, M. Kawasumi, A. Okada, Y. Fukushima, T. Kurauchi and O. Kamigaito, *J. Mater. Res.*, 2011, **8**, 1179–1184.
- A. Gupta, T. Sakthivel and S. Seal, *Prog. Mater. Sci.*, 2015, **73**, 44–126.
- M. Terrones, A. R. Botello-Mendez, J. Campos-Delgado, F. Lopez-Urias, Y. I. Vega-Cantu, F. J. Rodriguez-Macias, A. L. Elias, E. Munoz-Sandoval, A. G. Cano-Marquez, J.-C. Charlier and H. Terrones, *Nano Today*, 2010, **5**, 351–372.
- E. Ruiz-Hitzky and B. Casal, *Nature*, 1978, **276**, 596–597.
- P. Aranda and E. Ruiz-Hitzky, *Chem. Mater.*, 1992, **4**, 1395–1403.
- M. Darder, M. Colilla and E. Ruiz-Hitzky, *Chem. Mater.*, 2003, **15**, 3774–3780.
- M. Faustini, L. Nicole, E. Ruiz-Hitzky and C. Sanchez, *Adv. Funct. Mater.*, 2018, **28**, 1704158.
- M. Ogawa and K. Kuroda, *Chem. Rev.*, 1995, **95**, 399–438.
- E. Ruiz-Hitzky, *Adv. Mater.*, 1993, **5**, 334–340.
- E. Ruiz-Hitzky, P. Aranda, M. Darder and M. Ogawa, *Chem. Soc. Rev.*, 2011, **40**, 801–828.
- K. Ariga, *Beilstein J. Nanotechnol.*, 2023, **14**, 434–453.
- V. Nicolosi, M. Chhowalla, M. G. Kanatzidis, M. S. Strano and J. N. Coleman, *Science*, 2013, **340**, 1226419.
- E. Ruiz-Hitzky and P. Aranda, *J. Sol-Gel Sci. Technol.*, 2013, **70**, 307–316.
- E. Ruiz-Hitzky, P. Aranda, M. Akkari, N. Khaorapapong and M. Ogawa, *Beilstein J. Nanotechnol.*, 2019, **10**, 1140–1156.
- E. Ruiz-Hitzky, P. Aranda and C. Belver, in *Manipulation of Nanoscale Materials*, ed. K. Ariga, The Royal Society of Chemistry, 2012, DOI: [10.1039/9781849734158-00087](https://doi.org/10.1039/9781849734158-00087).
- M. Naguib, M. Kurtoglu, V. Presser, J. Lu, J. Niu, M. Heon, L. Hultman, Y. Gogotsi and M. W. Barsoum, *Adv. Mater.*, 2011, **23**, 4248–4253.
- B. Anasori and Y. Gogotsi, *2D Metal Carbides and Nitrides (MXenes): Structure, Properties and Applications*, Springer International Publishing, Cham, 2019.
- M. Naguib, V. N. Mochalin, M. W. Barsoum and Y. Gogotsi, *Adv. Mater.*, 2014, **26**, 992–1005.
- B. Anasori, M. R. Lukatskaya and Y. Gogotsi, *Nat. Rev. Mater.*, 2017, **2**, 9224.
- S. Ramanavicius and A. Ramanavicius, *Int. J. Mol. Sci.*, 2020, **21**, 9224.
- Y. Wang, Z. Niu, Y. Dai, P. Mu and J. Li, *Nanoscale*, 2023, **15**, 4170–4194.
- M. Ghidui, M. R. Lukatskaya, M. Q. Zhao, Y. Gogotsi and M. W. Barsoum, *Nature*, 2014, **516**, 78–81.
- M. Naguib, Engineering Electrically Conductive Clay-Like MXenes for Energy Storage, in *Program and Abstracts Book, 60th Annual Meeting, The Clay Minerals Society*, Austin, TX, USA, 2023.
- F. Bergaya and G. Lagaly, in *Developments in Clay Science*, ed. F. Bergaya and G. Lagaly, Elsevier, 2013, vol. 1, ch. General Introduction: Clays, Clay Minerals, and Clay Science.
- D. Zhang, C.-H. Zhou, C.-X. Lin, D.-S. Tong and W.-H. Yu, *Appl. Clay Sci.*, 2010, **50**, 1–11.
- H. Kodama and R. E. Grim, Encyclopedia Britannica, “clay mineral”, <https://www.britannica.com/science/clay-mineral>, (accessed 22nd June 2023).
- K. Momma and F. Izumi, *J. Appl. Crystallogr.*, 2011, **44**, 1272–1276.
- R. A. de Freitas and F. Wypych, in *Developments in Clay Science*, ed. F. Bergaya and G. Lagaly, Elsevier, 2022, vol. 10, pp. 253–275.
- D. Kim, R. F. Smith, I. K. Ocampo, F. Coppari, M. C. Marshall, M. K. Ginnane, J. K. Wicks, S. J. Tracy, M. Millot, A. Lazicki, J. R. Rygg, J. H. Eggert and T. S. Duffy, *Nat. Commun.*, 2022, **13**, 2260.
- C. E. Shuck, K. Ventura-Martinez, A. Goad, S. Uzun, M. Shekhirev and Y. Gogotsi, *ACS Chem. Health Saf.*, 2021, **28**, 326–338.
- A. Maughan, Porous two-dimensional materials (MXenes) for high capacity energy storage, PhD thesis, University of Lancaster, 2019.
- J. Chen, Y. Ding, D. Yan, J. Huang and S. Peng, *SusMat*, 2022, **2**, 293–318.
- J. Xu, T. Peng, X. Qin, Q. Zhang, T. Liu, W. Dai, B. Chen, H. Yu and S. Shi, *J. Mater. Chem. A*, 2021, **9**, 14147–14171.
- L. Liu, M. Orbay, S. Luo, S. Duluard, H. Shao, J. Harmel, P. Rozier, P.-L. Taberna and P. Simon, *ACS Nano*, 2022, **16**, 111–118.



- 41 N. H. Solangi, R. R. Karri, S. A. Mazari, N. M. Mubarak, A. S. Jatoti, G. Malafaia and A. K. Azad, *Coord. Chem. Rev.*, 2023, **477**, 214965.
- 42 T. Li, L. Yao, Q. Liu, J. Gu, R. Luo, J. Li, X. Yan, W. Wang, P. Liu, B. Chen, W. Zhang, W. Abbas, R. Naz and D. Zhang, *Angew. Chem., Int. Ed.*, 2018, **57**, 6115–6119.
- 43 J. Xuan, Z. Wang, Y. Chen, D. Liang, L. Cheng, X. Yang, Z. Liu, R. Ma, T. Sasaki and F. Geng, *Angew. Chem., Int. Ed.*, 2016, **55**, 14569–14574.
- 44 J. Santaren, J. Sanz and E. Ruiz-Hitzky, *Clays Clay Miner.*, 1990, **38**, 63–68.
- 45 V. Natu, R. Pai, M. Sokol, M. Carey, V. Kalra and M. W. Barsoum, *Chem*, 2020, **6**, 616–630.
- 46 S. Husmann, Ö. Budak, H. Shim, K. Liang, M. Aslan, A. Kruth, A. Quade, M. Naguib and V. Presser, *Chem. Commun.*, 2020, **56**, 11082–11085.
- 47 Z. Sun, M. Yuan, L. Lin, H. Yang, C. Nan, H. Li, G. Sun and X. Yang, *ACS Mater. Lett.*, 2019, **1**, 628–632.
- 48 D. Voiry, A. Mohite and M. Chhowalla, *Chem. Soc. Rev.*, 2015, **44**, 2702–2712.
- 49 E. Ruiz-Hitzky, B. Casal, P. Aranda and J. C. Galvan, *Rev. Inorg. Chem.*, 2001, **21**, 125–159.
- 50 K. D. Rasamani, F. Alimohammadi and Y. G. Sun, *Mater. Today*, 2017, **20**, 83–91.
- 51 G. D. Williams, N. T. Skipper, M. V. Smalley, A. K. Soper and S. M. King, *Faraday Discuss.*, 1996, **104**, 295–306.
- 52 J. A. Rausell-Colom, J. Saez-Auñón and C. H. Pons, *Clay Miner.*, 2018, **24**, 459–478.
- 53 S. Li, B. Gu, X. Li, S. Tang, L. Zheng, E. Ruiz-Hitzky, Z. Sun, C. Xu and X. Wang, *Adv. Healthcare Mater.*, 2022, **11**, 2102367.
- 54 X. Zuo, D. Wang, S. Zhang, Q. Liu and H. Yang, *Minerals*, 2018, **8**, 112.
- 55 J. I. Dawson, J. M. Kanczler, X. B. Yang, G. S. Attard and R. O. C. Oreffo, *Adv. Mater.*, 2011, **23**, 3304–3308.
- 56 A. Gholamipour-Shirazi, M. S. Carvalho, M. F. G. Huila, K. Araki, P. Dommersnes and J. O. Fossum, *Sci. Rep.*, 2016, **6**, 37239.
- 57 Y. Lvov, W. Wang, L. Zhang and R. Fakhrullin, *Adv. Mater.*, 2016, **28**, 1227–1250.
- 58 P. Mongondry, J. F. Tassin and T. Nicolai, *J. Colloid Interface Sci.*, 2005, **283**, 397–405.
- 59 J.-M. Oh, D.-H. Park, S.-J. Choi and J.-H. Choy, *Recent Pat. Nanotechnol.*, 2012, **6**, 200–217.
- 60 G. M. Bekaroglu and S. İşçi, *ACS Omega*, 2022, **7**, 38825–38831.
- 61 M. Rautureau, C. d. S. Figueiredo Gomes, N. Liewig and M. Katouzian-Safadi, *Clays and Health: Properties and Therapeutic Uses*, Springer Cham, 2017.
- 62 E. Ruiz-Hitzky, M. Darder, B. Wicklein, F. A. Castro-Smirnov and P. Aranda, *Clays Clay Miner.*, 2019, **67**, 44–58.
- 63 E. Ruiz-Hitzky, C. Ruiz-Garcia, F. M. Fernandes, G. Lo Dico, L. Lisuzzo, V. Prevot, M. Darder and P. Aranda, *Front. Chem.*, 2021, **9**, 733105.
- 64 S. Huang and V. N. Mochalin, *Inorg. Chem.*, 2019, **58**, 1958–1966.
- 65 P. Fulignati, *Minerals*, 2020, **10**, 919.
- 66 R. T. Cygan, J. A. Greathouse, H. Heinz and A. G. Kalinichev, *J. Mater. Chem.*, 2009, **19**, 2470–2481.
- 67 T. Wu and D.-e. Jiang, *MRS Bull.*, 2023, **48**, 253–260.
- 68 S. Srivatsa, P. Pačko, L. Mishnaevsky, T. Uhl and K. Grabowski, *Minerals*, 2020, **13**, 5189.
- 69 B. Biswas, B. Sarkar, R. Rusmin and R. Naidu, *Environ. Int.*, 2015, **85**, 168–181.
- 70 T. J. Pinnavaia, *Science*, 1983, **220**, 365–371.
- 71 J. F. Wang, J. Merino, P. Aranda, J. C. Galvan and E. Ruiz-Hitzky, *J. Mater. Chem.*, 1999, **9**, 161–168.
- 72 B. K. Singh and W. Um, *Minerals*, 2023, **13**, 239.
- 73 N. Boukhalifa, M. Darder, M. Boutahala, P. Aranda and E. Ruiz-Hitzky, *Bull. Chem. Soc. Jpn.*, 2021, **94**, 122–132.
- 74 Y. González-Alfaro, P. Aranda, F. M. Fernandes, B. Wicklein, M. Darder and E. Ruiz-Hitzky, *Adv. Mater.*, 2011, **23**, 5224–5228.
- 75 A. Sanguanwong, A. E. Flood, M. Ogawa, R. Martín-Sampedro, M. Darder, B. Wicklein, P. Aranda and E. Ruiz-Hitzky, *J. Hazard. Mater.*, 2021, **417**, 126068.
- 76 M. B. Ahmed, J. L. Zhou, H. H. Ngo and W. Guo, *Sci. Total Environ.*, 2015, **532**, 112–126.
- 77 J. Herney-Ramirez, M. A. Vicente and L. M. Madeira, *Appl. Catal., B*, 2010, **98**, 10–26.
- 78 G. Rytwo, *Sci. World J.*, 2012, 1–7, DOI: [10.1100/2012/498503](https://doi.org/10.1100/2012/498503).
- 79 G. Rytwo, *Abstracts of Papers of the American Chemical Society*, 2012, p. 243.
- 80 A. Khosla, H. T. A. A. Sonu, K. Singh, Gaurav, R. Walvekar, Z. Zhao, A. Kaushik, M. Khalid and V. Chaudhary, *Adv. Sci.*, 2022, **9**, 2203527.
- 81 C. Peng, X. Yang, Y. Li, H. Yu, H. Wang and F. Peng, *ACS Appl. Mater. Interfaces*, 2016, **8**, 6051–6060.
- 82 J. Low, L. Zhang, T. Tong, B. Shen and J. Yu, *J. Catal.*, 2018, **361**, 255–266.
- 83 Y. Sun and Y. Li, *Environ. Pollut.*, 2021, **278**, 116861.
- 84 L. Wang and Y.-L. Liu, *Crystals*, 2023, **13**(5), 804.
- 85 E. A. Hussein, M. M. Zagho, G. K. Nasrallah and A. A. Elzatahry, *Int. J. Nanomed.*, 2018, **13**, 2897–2906.
- 86 F. Liu, Z. Hu, M. Xiang and B. Hu, *Appl. Surf. Sci.*, 2022, **601**, 154227.
- 87 Z.-K. Li, Y. Liu, L. Li, Y. Wei, J. Caro and H. Wang, *J. Membr. Sci.*, 2019, **592**, 117361.
- 88 P.-L. Wang, C. Ma, Q. Yuan, T. Mai and M.-G. Ma, *J. Colloid Interface Sci.*, 2022, **606**, 971–982.
- 89 Y. Ibrahim, A. Kassab, K. Eid, A. M. Abdullah, K. I. Ozoemena and A. Elzatahry, *Nanomaterials*, 2020, **10**, 885.
- 90 M. Tawalbeh, S. Mohammed, A. Al-Othman, M. Yusuf, M. Mofijur and H. Kamyab, *Environ. Res.*, 2023, **228**, 115919.
- 91 T. Zhang, H. Bai, Y. Zhao, B. Ren, T. Wen, L. Chen, S. Song and S. Komarneni, *ACS Nano*, 2022, **16**, 4930–4939.



- 92 M. Darder, P. Aranda, A. I. Ruiz, F. M. Fernandes and E. Ruiz-Hitzky, *Mater. Sci. Technol.*, 2008, **24**, 1100–1110.
- 93 M. Darder, M. Colilla and E. Ruiz-Hitzky, *Chem. Mater.*, 2003, **15**, 3774–3780.
- 94 M. Darder, M. Colilla and E. Ruiz-Hitzky, *Appl. Clay Sci.*, 2005, **28**, 199–208.
- 95 E. Ruiz-Hitzky, *Chem. Rec.*, 2003, **3**, 88–100.
- 96 E. Ruiz-Hitzky, M. M. C. Sobral, A. Gomez-Aviles, C. Nunes, C. Ruiz-Garcia, P. Ferreira and P. Aranda, *Adv. Funct. Mater.*, 2016, **26**, 7394–7405.
- 97 S. Letaïef, P. Aranda and E. Ruiz-Hitzky, *Appl. Clay Sci.*, 2005, **28**, 183–198.
- 98 S. Letaïef, P. Aranda, R. Fernández-Saavedra, J. C. Margeson, C. Detellier and E. Ruiz-Hitzky, *J. Mater. Chem.*, 2008, **18**, 2227–2233.
- 99 A. Barra, C. Nunes, E. Ruiz-Hitzky and P. Ferreira, *Int. J. Mol. Sci.*, 2022, **23**, 1848.
- 100 M. Darder, P. Aranda, C. Ruiz-Garcia, F. M. Fernandes and E. Ruiz-Hitzky, *Adv. Funct. Mater.*, 2018, **28**, 1704323.
- 101 J.-M. Yeh, S.-J. Liou, C.-Y. Lai, P.-C. Wu and T.-Y. Tsai, *Chem. Mater.*, 2001, **13**, 1131–1136.
- 102 M. Ghidui, J. Halim, S. Kota, D. Bish, Y. Gogotsi and M. W. Barsoum, *Chem. Mater.*, 2016, **28**, 3507–3514.
- 103 E. Wang, Y. Cao, Y. Bai, Y. Gai, Y. Shan, Q. Li, T. Jiang, H. Feng and Z. Li, *J. Micromech. Microeng.*, 2022, **32**, 044003.
- 104 Z. Huang, S. Wang, S. Kota, Q. Pan, M. W. Barsoum and C. Y. Li, *Polymer*, 2016, **102**, 119–126.
- 105 U. Noor, M. F. Mughal, T. Ahmed, M. F. Farid, M. Ammar, U. Kulsum, A. Saleem, M. Naeem, A. Khan, A. Sharif and K. Waqar, *Nanotechnology*, 2023, **34**, 262001.
- 106 Z. Zhou, W. Panatdasirisuk, T. S. Mathis, B. Anasori, C. Lu, X. Zhang, Z. Liao, Y. Gogotsi and S. Yang, *Nanoscale*, 2018, **10**, 6005–6013.
- 107 X. Feng, J. Huang, J. Ning, D. Wang, J. Zhang and Y. Hao, *Carbon*, 2023, **205**, 365–372.
- 108 F. Shahzad, M. Alhabeab, C. B. Hatter, B. Anasori, S. Man Hong, C. M. Koo and Y. Gogotsi, *Science*, 2016, **353**, 1137–1140.
- 109 J. Liu, H.-B. Zhang, R. Sun, Y. Liu, Z. Liu, A. Zhou and Z.-Z. Yu, *Adv. Mater.*, 2017, **29**, 1702367.
- 110 H. Yan, L. Zhang, H. Li, X. Fan and M. Zhu, *Carbon*, 2020, **157**, 217–233.
- 111 H. Zhao, J. Ding, M. Zhou and H. Yu, *ACS Appl. Nano Mater.*, 2021, **4**, 3075–3086.
- 112 P. D. Kaviratna, T. J. Pinnavaia and P. A. Schroeder, *J. Phys. Chem. Solids*, 1996, **57**, 1897–1906.
- 113 V. Tomer, G. Polizos, C. A. Randall and E. Manias, *J. Appl. Phys.*, 2011, **109**, 074113.
- 114 D. T. Rathnayake, K. S. P. Karunadasa, A. S. K. Wijekoon, C. H. Manoratne and R. M. G. Rajapakse, *Chem. Pap.*, 2022, **76**, 6653–6658.
- 115 Y. S. Choi, T. K. Kim, E. A. Kim, S. H. Joo, C. Pak, Y. H. Lee, H. Chang and D. Seung, *Adv. Mater.*, 2008, **20**, 2341–2344.
- 116 C. Tang, K. Hackenberg, Q. Fu, P. M. Ajayan and H. Ardebili, *Nano Lett.*, 2012, **12**, 1152–1156.
- 117 C. Ruiz-Garcia, R. Jimenez, J. Perez-Carvajal, A. Berenguer-Murcia, M. Darder, P. Aranda, D. Cazorla-Amoros and E. Ruiz-Hitzky, *Sci. Adv. Mater.*, 2014, **6**, 151–158.
- 118 S. Maiti, A. Pramanik, S. Chattopadhyay, G. De and S. Mahanty, *J. Colloid Interface Sci.*, 2016, **464**, 73–82.
- 119 S.-S. Chai, W.-B. Zhang, J.-L. Yang, L. Zhang, X.-W. Han, M. M. Theint and X.-J. Ma, *J. Rare Earths*, 2023, **41**, 728–739.
- 120 M. R. Lukatskaya, O. Mashtalir, C. E. Ren, Y. Dall'Agnese, P. Rozier, P. L. Taberna, M. Naguib, P. Simon, M. W. Barsoum and Y. Gogotsi, *Science*, 2013, **341**, 1502–1505.
- 121 R. B. Rakhi, B. Ahmed, M. N. Hedhili, D. H. Anjum and H. N. Alshareef, *Chem. Mater.*, 2015, **27**, 5314–5323.
- 122 A. Enaiet Allah, *RSC Adv.*, 2023, **13**, 9983–9997.
- 123 S. Qamar, K. Fatima, N. Ullah, Z. Akhter, A. Waseem and M. Sultan, *Nanoscale*, 2022, **14**, 13018–13039.
- 124 S. Sarikurt, D. Çakır, M. Keçeli and C. Sevik, *Nanoscale*, 2018, **10**, 8859–8868.
- 125 Z. Fan, Y. Wang, Z. Xie, X. Xu, Y. Yuan, Z. Cheng and Y. Liu, *Nanoscale*, 2018, **10**, 9642–9652.
- 126 J. Pang, R. G. Mendes, A. Bachmatiuk, L. Zhao, H. Q. Ta, T. Gemming, H. Liu, Z. Liu and M. H. Rummeli, *Chem. Soc. Rev.*, 2019, **48**, 72–133.
- 127 D. Parajuli, N. Murali, K. C. Devendra, B. Karki, K. Samatha, A. A. Kim, M. Park and B. Pant, *Polymers*, 2022, **14**, 3433.
- 128 B. Szczepanik, *Appl. Clay Sci.*, 2017, **141**, 227–239.
- 129 E. Ruiz-Hitzky, P. Aranda, M. Darder and G. Rytwo, *J. Mater. Chem.*, 2010, **20**, 9306–9321.
- 130 T. Hoang-Minh, T. L. Le, J. Kasbohm and R. Gieré, *Appl. Clay Sci.*, 2010, **48**, 349–357.
- 131 L. Margulies, H. Rozen and E. Cohen, *Nature*, 1985, **315**, 658–659.
- 132 K. Gopalram, A. Kapoor, P. S. Kumar, A. Sunil and G. Rangasamy, *Ind. Eng. Chem. Res.*, 2023, **62**, 6559–6583.
- 133 H. Jiang, S. Zhang, X. Feng, S. Yin and W. Zhao, *Processes*, 2023, **11**, 1413.
- 134 Z. Guo, J. Zhou, L. Zhu and Z. Sun, *J. Mater. Chem. A*, 2016, **4**, 11446–11452.
- 135 T. Lan and T. J. Pinnavaia, *Chem. Mater.*, 1994, **6**, 2216–2219.
- 136 P. Kiliaris and C. D. Papaspyrides, *Prog. Polym. Sci.*, 2010, **35**, 902–958.
- 137 J. M. Garcés, D. J. Moll, J. Bicerano, R. Fibiger and D. G. McLeod, *Adv. Mater.*, 2000, **12**, 1835–1839.
- 138 S. Gul, A. Kausar, B. Muhammad and S. Jabeen, *Polym.-Plast. Technol. Eng.*, 2016, **55**, 684–703.
- 139 M. Okamoto and B. John, *Prog. Polym. Sci.*, 2013, **38**, 1487–1503.
- 140 M. Darder, P. Aranda and E. Ruiz-Hitzky, *Adv. Mater.*, 2007, **19**, 1309–1319.
- 141 S. Sinha Ray, P. Maiti, M. Okamoto, K. Yamada and K. Ueda, *Macromolecules*, 2002, **35**, 3104–3110.



- 142 M. Wasim, F. Shi, J. Liu, H. Zhang, K. Zhu and Z. Tian, *J. Polym. Res.*, 2022, **29**, 423.
- 143 S. Tang, Z. Wu, X. Li, F. Xie, D. Ye, E. Ruiz-Hitzky, L. Wei and X. Wang, *Carbohydr. Polym.*, 2023, **299**, 120204.
- 144 H. Zhang, L. Wang, Q. Chen, P. Li, A. Zhou, X. Cao and Q. Hu, *Mater. Des.*, 2016, **92**, 682–689.
- 145 L. Li, X. Liu, J. Wang, Y. Yang, Y. Cao and W. Wang, *Composites, Part A*, 2019, **127**, 105649.
- 146 V. Chaudhary, A. Gautam, Y. K. Mishra and A. Kaushik, *Nanomaterials*, 2021, **11**, 2496.
- 147 Y. Wang, Y. Yue, F. Cheng, Y. Cheng, B. Ge, N. Liu and Y. Gao, *ACS Nano*, 2022, **16**, 1734–1758.
- 148 L. Wei, Z. Wu, S. Tang, X. Qin, Y. Xiong, J. Li, E. Ruiz-Hitzky and X. Wang, *Carbon*, 2023, **203**, 386–396.
- 149 S. Tang, Z. Wu, G. Feng, L. Wei, J. Weng, E. Ruiz-Hitzky and X. Wang, *Chem. Eng. J.*, 2023, **454**, 140457.
- 150 R. Li, L. Zhang, L. Shi and P. Wang, *ACS Nano*, 2017, **11**, 3752–3759.
- 151 S. M. George and B. Kandasubramanian, *Ceram. Int.*, 2020, **46**, 8522–8535.
- 152 H. Riazi, S. K. Nemani, M. C. Grady, B. Anasori and M. Soroush, *J. Mater. Chem. A*, 2021, **9**, 8051–8098.
- 153 Y. Shen, W. Yang, F. Hu, X. Zheng, Y. Zheng, H. Liu, H. Algadi and K. Chen, *Adv. Compos. Hybrid Mater.*, 2022, **6**, 21.
- 154 T. Undabeytia, U. Shuali, S. Nir and B. Rubin, *Minerals*, 2021, **11**, 9.
- 155 T. Undabeytia, S. Nir, E. Tel-Or and B. Rubin, *J. Agric. Food Chem.*, 2000, **48**, 4774–4779.
- 156 M. Nuruzzaman, M. M. Rahman, Y. Liu and R. Naidu, *J. Agric. Food Chem.*, 2016, **64**, 1447–1483.
- 157 G. Rytwo, R. Lavi, Y. Rytwo, H. Monchase, S. Dultz and T. N. König, *Sci. Total Environ.*, 2013, **442**, 134–142.
- 158 S. L. Lemke, P. G. Grant and T. D. Phillips, *J. Agric. Food Chem.*, 1998, **46**, 3789–3796.
- 159 Y. Fu, W. C. Wang, L. Q. Zhang, V. Vinokurov, A. Stavitskaya and Y. Lvov, *Materials*, 2019, **12**, 4195.
- 160 S. Song, X. Jiang, H. Shen, W. Wu, Q. Shi, M. Wan, J. Zhang, H. Mo and J. Shen, *ACS Appl. Bio Mater.*, 2021, **4**, 6912–6923.
- 161 J. Singhal, S. Verma and S. Kumar, *Sci. Total Environ.*, 2022, **837**, 155669.
- 162 C. Aguzzi, P. Cerezo, C. Viseras and C. Caramella, *Appl. Clay Sci.*, 2007, **36**, 22–36.
- 163 E. Ruiz-Hitzky, M. Darder, B. Wicklein, F. M. Fernandes, F. A. Castro-Smirnov, M. A. M. del Burgo, G. del Real and P. Aranda, Advanced biohybrid materials based on nanoclays for biomedical applications, Incheon, South Korea, 2012.
- 164 E. E. Gaskell and A. R. Hamilton, *Future Med. Chem.*, 2014, **6**, 641–655.
- 165 M. Long, Y. Zhang, P. Huang, S. Chang, Y. H. Hu, Q. Yang, L. F. Mao and H. M. Yang, *Adv. Funct. Mater.*, 2018, **28**, 1704452.
- 166 P. Irvani, S. Irvani and R. S. Varma, *Micromachines*, 2022, **13**, 1383.
- 167 M. Soleymaniha, M.-A. Shahbazi, A. R. Rafieerad, A. Maleki and A. Amiri, *Adv. Healthcare Mater.*, 2019, **8**, 1801137.
- 168 H. Li, J. Dai, X. Yi and F. Cheng, *Biomater. Adv.*, 2022, **140**, 213055.
- 169 G. Liu, J. Zou, Q. Tang, X. Yang, Y. Zhang, Q. Zhang, W. Huang, P. Chen, J. Shao and X. Dong, *ACS Appl. Mater. Interfaces*, 2017, **9**, 40077–40086.
- 170 H. Lin, X. Wang, L. Yu, Y. Chen and J. Shi, *Nano Lett.*, 2017, **17**, 384–391.
- 171 S. Kumar, Y. Lei, N. H. Alshareef, M. A. Quevedo-Lopez and K. N. Salama, *Biosens. Bioelectron.*, 2018, **121**, 243–249.
- 172 L. S. Pires, F. D. Magalhães and A. M. Pinto, *Polymers*, 2022, **14**, 1464.
- 173 C. R. Smith, *J. Am. Chem. Soc.*, 1934, **56**, 1561–1563.
- 174 J. E. Gieseking, *Soil Sci.*, 1939, **47**, 1–14.
- 175 S. B. Hendricks, *J. Phys. Chem.*, 1941, **45**, 65–81.
- 176 E. Ruiz-Hitzky, P. Aranda and M. Darder, in *Tailored Organic–Inorganic Materials*, ed. J. L. C. A. C. E. Brunet, 2015, ch. 6, pp. 245–297, DOI: [10.1002/9781118792223.ch6](https://doi.org/10.1002/9781118792223.ch6).
- 177 E. Ruiz-Hitzky, P. Aranda and M. J. Serratos, in *Handbook of Layered Materials*, ed. S. M. Auerbach, K. A. Carrado and P. K. Dutta, Taylor & Francis Group, New York, 2004, ch. 3, pp. 91–154.
- 178 M. Naguib, V. N. Mochalin, Y. Dall'Agnese, M. Heon, M. W. Barsoum and Y. Gogotsi, *Nat. Commun.*, 2013, **4**, 1716.
- 179 S. H. Overbury, A. I. Kolesnikov, G. M. Brown, Z. Y. Zhang, G. S. Nair, R. L. Sacci, R. Lotfi, A. C. T. van Duin and M. Naguib, *J. Am. Chem. Soc.*, 2018, **140**, 10305–10314.
- 180 G. W. Brindley and R. E. Sempels, *Clay Miner.*, 1977, **12**, 229–237.
- 181 A. M. de Andres, J. Merino, J. C. Galvan and E. Ruiz-Hitzky, *Mater. Res. Bull.*, 1999, **34**, 641–651.
- 182 D. Plee, F. Borg, L. Gatineau and J. J. Fripiat, *J. Am. Chem. Soc.*, 1985, **107**, 2362–2369.
- 183 A. Schutz, W. E. E. Stone, G. Poncelet and J. J. Fripiat, *Clays Clay Miner.*, 1987, **35**, 251–262.
- 184 W. Jones, G. Poncelet, E. Ruiz-Hitzky, P. Pomonis, H. Van Damme, F. Bergaya and N. Papayannakos, Synthesis, Characterisation and Application of Pillared Clays Produced in Large Quantities Brite, <https://www.jmg.ch.cam.ac.uk/resources/pages/wj/index.html> (accessed 4th of March, 2023).
- 185 J. Zhu, L. Wang, J. Wang, F. Wang, M. Tian, S. Zheng, N. Shao, L. Wang and M. He, *ACS Nano*, 2020, **14**, 15306–15316.
- 186 T. Endo, M. M. Mortland and T. J. Pinnavaia, *Clays Clay Miner.*, 1980, **28**, 105–110.
- 187 J. Ahenach, P. Cool, R. E. N. Impens and E. F. Vansant, *J. Porous Mater.*, 2000, **7**, 475–481.
- 188 Y.-S. Han, H. Matsumoto and S. Yamanaka, *Chem. Mater.*, 1997, **9**, 2013–2018.
- 189 A. Moini and T. J. Pinnavaia, *Solid State Ionics*, 1988, **26**, 119–123.



- 190 S. Letaief and E. Ruiz-Hitzky, *Chem. Commun.*, 2003, 2996–2997, DOI: [10.1039/b310854f](https://doi.org/10.1039/b310854f).
- 191 S. Letaief, M. A. Martín-Luengo, P. Aranda and E. Ruiz-Hitzky, *Adv. Funct. Mater.*, 2006, **16**, 401–409.
- 192 P. A. Maughan, V. R. Seymour, R. Bernardo-Gavito, D. J. Kelly, S. Shao, S. Tantisriyanurak, R. Dawson, S. J. Haigh, R. J. Young, N. Tapia-Ruiz and N. Bimbo, *Langmuir*, 2020, **36**, 4370–4382.
- 193 E. Manova, P. Aranda, M. A. Martín-Luengo, S. Letaief and E. Ruiz-Hitzky, *Microporous Mesoporous Mater.*, 2010, **131**, 252–260.
- 194 S. Yamanaka, T. Nishihara, M. Hattori and Y. Suzuki, *Mater. Chem. Phys.*, 1987, **17**, 87–101.
- 195 E. G. Rightor, M. S. Tzou and T. J. Pinnavaia, *J. Catal.*, 1991, **130**, 29–40.
- 196 M. Akkari, P. Aranda, H. Ben Rhaïem, A. Ben Haj Amara and E. Ruiz-Hitzky, *Appl. Clay Sci.*, 2016, **131**, 131–139.
- 197 G. W. Brindley and S. Yamanaka, *Am. Mineral.*, 1979, **64**, 830–835.
- 198 S. Zhang, H. Ying, P. Huang, J. Wang, Z. Zhang, T. Yang and W.-Q. Han, *ACS Nano*, 2020, **14**, 17665–17674.
- 199 X. Qin, Z. Wu, J. Fang, S. Li, S. Tang and X. Wang, *Appl. Surf. Sci.*, 2023, **616**, 156521.
- 200 J. Lipton, G.-M. Weng, M. Alhabeab, K. Maleski, F. Antonio, J. Kong, Y. Gogotsi and A. D. Taylor, *Nanoscale*, 2019, **11**, 20295–20300.
- 201 A. C. Longden, *Phys. Rev.*, 1902, **15**, 355–365.
- 202 C. Ruiz-García, F. Heras, M. Á. Gilarranz, P. Aranda and E. Ruiz-Hitzky, *Appl. Clay Sci.*, 2018, **161**, 132–138.
- 203 W. D. Zhang, I. Y. Phang and T. X. Liu, *Adv. Mater.*, 2006, **18**, 73–77.
- 204 P. Aranda and E. Ruiz-Hitzky, *Chem. Rec.*, 2018, **18**, 1125–1137.
- 205 S.-N. Ding, C.-L. Zheng, N. Wan and S. Cosnier, *Monatsh. Chem. – Chem. Mon.*, 2014, **145**, 1389–1394.
- 206 Y.-F. Lan and J.-J. Lin, *J. Phys. Chem. A*, 2009, **113**, 8654–8659.
- 207 Z. Wang, X. Meng, J. Li, X. Du, S. Li, Z. Jiang and T. Tang, *J. Phys. Chem. C*, 2009, **113**, 8058–8064.
- 208 F. M. Fernandes and E. Ruiz-Hitzky, *Carbon*, 2014, **72**, 296–303.
- 209 T. Kyotani, N. Sonobe and A. Tomita, *Nature*, 1988, **331**, 331–333.
- 210 N. Sonobe, T. Kyotani, Y. Hishiyama, M. Shiraishi and A. Tomita, *J. Phys. Chem.*, 1988, **92**, 7029–7034.
- 211 N. Sonobe, T. Kyotani and A. Tomita, *Carbon*, 1988, **26**, 573–578.
- 212 M. Darder and E. R. Ruiz-Hitzky, *J. Mater. Chem.*, 2005, **15**, 3913–3918.
- 213 C. Ruiz-García, J. Perez-Carvajal, A. Berenguer-Murcia, M. Darder, P. Aranda, D. Cazorla-Amoros and E. Ruiz-Hitzky, *Phys. Chem. Chem. Phys.*, 2013, **15**, 18635–18641.
- 214 R. Fernández-Saavedra, P. Aranda and E. Ruiz-Hitzky, *Adv. Funct. Mater.*, 2004, **14**, 77–82.
- 215 A. Gomez-Aviles, M. Darder, P. Aranda and E. Ruiz-Hitzky, *Angew. Chem., Int. Ed.*, 2007, **46**, 923–925.
- 216 E. Ruiz-Hitzky, M. Darder, F. M. Fernandes, E. Zatile, F. J. Palomares and P. Aranda, *Adv. Mater.*, 2011, **23**, 5250–5255.
- 217 C. Xu, G. Ning, X. Zhu, G. Wang, X. Liu, J. Gao, Q. Zhang, W. Qian and F. Wei, *Carbon*, 2013, **62**, 213–221.
- 218 A. Barra, J. D. C. Santos, M. R. F. Silva, C. Nunes, E. Ruiz-Hitzky, I. Gonçalves, S. Yildirim, P. Ferreira and P. A. A. P. Marques, *Nanomaterials*, 2020, **10**, 2077.
- 219 A. S. Levitt, M. Alhabeab, C. B. Hatter, A. Sarycheva, G. Dion and Y. Gogotsi, *J. Mater. Chem. A*, 2019, **7**, 269–277.
- 220 X. Li, X. Yin, M. Han, C. Song, H. Xu, Z. Hou, L. Zhang and L. Cheng, *J. Mater. Chem. C*, 2017, **5**, 4068–4074.
- 221 B. Dai, B. Zhao, X. Xie, T. Su, B. Fan, R. Zhang and R. Yang, *J. Mater. Chem. C*, 2018, **6**, 5690–5697.
- 222 J. Rajendran, T. S. Kannan, L. S. Dhanasekaran, P. Murugan, R. Atchudan, Z. A. Allothman, M. Ouladsmame and A. K. Sundramoorthy, *Chemosphere*, 2022, **287**, 132106.
- 223 X. Xie, M.-Q. Zhao, B. Anasori, K. Maleski, C. E. Ren, J. Li, B. W. Byles, E. Pomerantseva, G. Wang and Y. Gogotsi, *Nano Energy*, 2016, **26**, 513–523.
- 224 P. Gao, H. Shi, T. Ma, S. Liang, Y. Xia, Z. Xu, S. Wang, C. Min and L. Liu, *ACS Appl. Mater. Interfaces*, 2021, **13**, 51028–51038.
- 225 Z. Wu, W. Deng, S. Tang, E. Ruiz-Hitzky, J. Luo and X. Wang, *Chem. Eng. J.*, 2021, **426**, 130776.
- 226 Y. Fukushima and S. Inagaki, *J. Inclusion Phenom.*, 1987, **5**, 473–482.
- 227 A. Okada, Y. Fukushima, M. Kawasumi, S. Inagaki, A. Usuki, S. Sugiyama, T. Kurauchi, O. Kamigaito, *USA Pat.*, 4739007, 1988.
- 228 E. Ruiz-Hitzky, P. Aranda and M. J. Serratos, in *Handbook of Layered Materials*, ed. S. M. Auerbach, K. A. Carrado and P. K. Dutta, Marcel Dekker, New York, 2004, p. 91.
- 229 A. Okada and A. Usuki, *Macromol. Mater. Eng.*, 2006, **291**, 1449–1476.
- 230 M. Carey and M. W. Barsoum, *Mater. Today Adv.*, 2021, **9**, 100120.
- 231 M. Carey, Z. Hinton, M. Sokol, N. J. Alvarez and M. W. Barsoum, *ACS Appl. Mater. Interfaces*, 2019, **11**, 20425–20436.
- 232 Y. J. Liu, D. C. Degroot, J. L. Schindler, C. R. Kannewurf and M. G. Kanatzidis, *Chem. Mater.*, 1991, **3**, 992–994.
- 233 E. Ruiz-Hitzky and P. Aranda, *Adv. Mater.*, 1990, **2**, 545–547.
- 234 E. Ruiz-Hitzky, P. Aranda, B. Casal and J. C. Galvan, *Adv. Mater.*, 1995, **7**, 180–184.
- 235 V. Mehrotra and E. P. Giannelis, *Solid State Commun.*, 1991, **77**, 155–158.
- 236 M. Boota, B. Anasori, C. Voigt, M.-Q. Zhao, M. W. Barsoum and Y. Gogotsi, *Adv. Mater.*, 2016, **28**, 1517–1522.
- 237 K. Li, J. Zhao, A. Zhussupbekova, C. E. Shuck, L. Hughes, Y. Dong, S. Barwich, S. Vaesen, I. V. Shvets, M. Möbius,



- W. Schmitt, Y. Gogotsi and V. Nicolosi, *Nat. Commun.*, 2022, **13**, 6884.
- 238 K. Li, X. Wang, S. Li, P. Urbankowski, J. Li, Y. Xu and Y. Gogotsi, *Small*, 2020, **16**, 1906851.
- 239 N. Lara and E. Ruiz-Hitzky, *J. Braz. Chem. Soc.*, 1996, **7**, 193–197.
- 240 M. G. Kanatzidis, C. G. Wu, H. O. Marcy and C. R. Kannewurf, *J. Am. Chem. Soc.*, 1989, **111**, 4139–4141.
- 241 E. Ruiz-Hitzky, P. Aranda and B. Casal, *J. Mater. Chem.*, 1992, **2**, 581–582.
- 242 C.-F. Du, X. Zhao, Z. Wang, H. Yu and Q. Ye, *Nanomaterials*, 2021, **11**, 166.
- 243 Q. Pan, Y. Zheng, S. Kota, W. Huang, S. Wang, H. Qi, S. Kim, Y. Tu, M. W. Barsoum and C. Y. Li, *Nanoscale Adv.*, 2019, **1**, 395–402.
- 244 C. Wang, Z. Zhang, J. Wang, Q. Wang and L. Shang, *Mater. Today Bio*, 2022, **16**, 100352.
- 245 E. Ruiz-Hitzky, P. Aranda and M. Darder, in *Kirk-Othmer Encyclopedia of Chemical Technology*, John Wiley & Sons, 2008, pp. 1–28. DOI: [10.1002/0471238961.bionruiz.a01](https://doi.org/10.1002/0471238961.bionruiz.a01).
- 246 V. Ojijo and S. Sinha Ray, *Prog. Polym. Sci.*, 2013, **38**, 1543–1589.
- 247 E. Ruiz-Hitzky, M. Darder, F. M. Fernandes, B. Wicklein, A. C. S. Alcântara and P. Aranda, *Prog. Polym. Sci.*, 2013, **38**, 1392–1414.
- 248 E. Ruiz-Hitzky, K. Ariga and Y. Lvov, *Bio-inorganic Hybrid Nanomaterials*, Wiley-VCH, 2007.
- 249 E. Ruiz-Hitzky, M. Darder and P. Aranda, *J. Mater. Chem.*, 2005, **15**, 3650–3662.
- 250 V. J. Cadarso, A. Llobera, C. Fernandez-Sanchez, M. Darder and C. Dominguez, *Sens. Actuators, B*, 2009, **139**, 143–149.
- 251 A. C. S. Alcântara, M. Darder, P. Aranda and E. Ruiz-Hitzky, *Appl. Clay Sci.*, 2014, **96**, 2–8.
- 252 Z. Tang, N. A. Kotov, S. Magonov and B. Ozturk, *Nat. Mater.*, 2003, **2**, 413–418.
- 253 K. Sung, S. Nakagawa and N. Yoshie, *ACS Omega*, 2017, **2**, 8475–8482.
- 254 M. M. González del Campo, M. Darder, P. Aranda, M. Akkari, Y. Huttel, A. Mayoral, J. Bettini and E. Ruiz-Hitzky, *Adv. Funct. Mater.*, 2018, **28**, 1703048.
- 255 F. A. Castro-Smirnov, J. Ayache, J.-R. Bertrand, E. Dardillac, E. Le Cam, O. Piétrement, P. Aranda, E. Ruiz-Hitzky and B. S. Lopez, *Sci. Rep.*, 2017, **7**, 5586.
- 256 F. A. Castro-Smirnov, O. Piétrement, P. Aranda, J.-R. Bertrand, J. Ayache, E. Le Cam, E. Ruiz-Hitzky and B. S. Lopez, *Sci. Rep.*, 2016, **6**, 36341.
- 257 V. M. Hong Ng, H. Huang, K. Zhou, P. S. Lee, W. Que, J. Z. Xu and L. B. Kong, *J. Mater. Chem. A*, 2017, **5**, 3039–3068.
- 258 C. I. Idumah, *International Journal of Polymeric Materials and Polymeric Biomaterials*, 2022, pp. 1–22, DOI: [10.1080/00914037.2022.2098297](https://doi.org/10.1080/00914037.2022.2098297).
- 259 M. Darder, P. Aranda, M. L. Ferrer, M. C. Gutiérrez, F. del Monte and E. Ruiz-Hitzky, *Adv. Mater.*, 2011, **23**, 5262–5267.
- 260 X. Li, Y.-C. Li, M. Chen, Q. Shi, R. Sun and X. Wang, *J. Mater. Chem. B*, 2018, **6**, 6544–6549.
- 261 H. Lin, Y. Chen and J. Shi, *Adv. Sci.*, 2018, **5**, 1800518.

